AL-TR-1991-0029

AD-A248 613

OPTIMAL ECG ELECTRODE SITES AND CRITERIA FOR DETECTION OF ASYMPTOMATIC CORONARY ARTERY DISEASE—UPDATE 1990

MULTILEAD ECG CHANGES AT REST, WITH EXERCISE, AND WITH CORONARY ANGIOPLASTY

Ronald H. Selvester[1,2]
Joseph C. Solomon[1,2]
Kesaag Baron[2]
Helge A. Saetre[2]
Myrvin H. Ellestad[2]

[1]University of Southern California, Rancho Campus
7601 E. Imperial Highway
Downey, CA 90242

[2]Memorial Heart Institute
Long Beach Memorial Medical Center Foundation
2801 Atlantic Avenue
Long Beach, CA 90801

DTIC
ELECTE
APR 03 1992
S B D

AEROSPACE MEDICINE DIRECTORATE
Brooks Air Force Base, TX 78235-5000

Southeastern Center for Electrical Engineering Education
Management Office, Central Florida Facility
11th & Massachusetts Avenues
St. Cloud, FL 32769

92-08428

February 1992

Final Technical Report for Period 1 June 1989 – 15 December 1990

Approved for public release; distribution is unlimited.

92 4 02 079

AIR FORCE SYSTEMS COMMAND
BROOKS AIR FORCE BASE, TEXAS 78235-5000

ARMSTRONG LABORATORY

NOTICES

When Government drawings, specifications, or other data are used for any purpose other than in connection with a definitely Government-related procurement, the United States Government incurs no responsibility or any obligation whatsoever. The fact that the Government may have formulated or in any way supplied the said drawings, specifications, or other data, is not to be regarded by implication, or otherwise in any manner construed, as licensing the holder or any other person or corporation; or as conveying any rights or permission to manufacture, use, or sell any patented invention that may in any way be related thereto.

The voluntary, fully informed consent of the subjects used in this research was obtained as required by AFR 169-6.

The Office of Public Affairs has reviewed this report, and it is releasable to the National Technical Information Service, where it will be available to the general public, including foreign nationals.

This report has been reviewed and is approved for publication.

R. Brian Howe

R. BRIAN HOWE, M.A.
Project Scientist

Gil D. Tolan

GIL D. TOLAN, Colonel, USAF, MC, CFS
Deputy, Research Operations

James R Hickman Jr

JAMES R. HICKMAN, JR., Colonel, USAF, MC
Chief, Clinical Sciences Division

REPORT DOCUMENTATION PAGE

Form Approved
OMB No. 0704-0188

Public reporting burden for this collection of information is estimated to average 1 hour per response, including the time for reviewing instructions, searching existing data sou and maintaining the data needed, and completing and reviewing the collection of information. Send comments regarding this burden estimate or any other aspect of th information, including suggestions for reducing this burden, to Washington Headquarters Services, Directorate for Information Operations and Reports, 1215 Jefferson Davis 1204, Arlington, VA 22202-4302, and to the Office of Management and Budget, Paperwork Reduction Project (0704-0188), Washington, DC 20503.

1. AGENCY USE ONLY (Leave blank)	2. REPORT DATE	3. REPORT TYPE AND DATES COVERED
	February 1992	Final – 1 June 1989 – 15 December 1990

4. TITLE AND SUBTITLE
Optimal ECG Electrode Sites and Criteria for Detection of Asymptomatic Coronary Artery Disease—Update 1990: Multilead ECG Changes at Rest, With Exercise, and With Coronary Angioplasty

5. FUNDING NUMBERS
C – F33615-87-D-0609/0023
PE – 62202F
PR – 7755
TA – 27
WU – 19

6. AUTHOR(S)
Ronald H. Selvester
Joseph C. Solomon
Kesaag Baron
Helge A. Saetre
Myrvin H. Ellestad

7. PERFORMING ORGANIZATION NAME(S) AND ADDRESS(ES)
University of Southern California,
Rancho Campus
7601 E. Imperial Highway
Downey, CA 90242

Memorial Heart Institute, Long Beach
Memorial Medical Center Foundation
2801 Atlantic Avenue
Long Beach, CA 90801

8. PERFORMING ORGANIZATION REPORT NUMBER

9. SPONSORING/MONITORING AGENCY NAMES(S) AND ADDRESS(ES)
Armstrong Laboratory
Aerospace Medicine Directorate
Brooks Air Force Base, TX 78235-5000

10. SPONSORING/MONITORING AGENCY REPORT NUMBER
AL-TR-1991-0029

11. SUPPLEMENTARY NOTES
Armstrong Laboratory Technical Monitor: R. Brian Howe, (512) 536-2285.
The software described on page 34 is available from the performing organization only.

12a. DISTRIBUTION/AVAILABILITY STATEMENT
Approved for public release; distribution is unlimited.

12b. DISTRIBUTION CODE

13. ABSTRACT (Maximum 200 words)

This report presents recent findings from the Selvester-Solomon forward model of the electrophysiology of the human heart simulating infarct and ischemia. This led to a study of a 16-lead ECG at the time of coronary angioplasty. Both the simulations and the angioplasty study (reported in detail in this report) provide evidence that routine screening of apparently healthy aircrews with Hi-Fi rest and exercise 30 lead ECGs will significantly improve the detection of asymptomatic coronary disease. Three ECG recording systems with signal processing of 30 simultaneous leads (30SL) have been developed. These systems record and store on disk up to 2 hr of continuous 3 lead rhythm strips and 10 s epochs of 30SL median beats sampled at 1 ms. Design documents, flow diagrams, schematics, and safety documentation for the 3 ECG mapping systems, and for 3 electrode locator systems designed and fabricated on this contract, are provided. The design of the study at Long Beach Memorial and Armstrong Laboratory is also presented for the follow-on 1 year's contract using 30SL data during exercise (and angioplasty) to define the optimal number of leads and criteria in them for the optimal detection of asymptomatic coronary disease in aircrew persons.

14. SUBJECT TERMS
Body surface map
Computer forward model
Coronary artery disease
Electrocardiography
Exercise tolerance test
Heart model
Myocardial infarction
Myocardial ischemia

15. NUMBER OF PAGES
66

16. PRICE CODE

17. SECURITY CLASSIFICATION OF REPORT	18. SECURITY CLASSIFICATION OF THIS PAGE	19. SECURITY CLASSIFICATION OF ABSTRACT	20. LIMITATION OF ABSTRACT
Unclassified	Unclassified	Unclassified	UL

NSN 7540-01-280-5500

Standard Form 298 (Rev. 2-89)
Prescribed by ANSI Std. Z39-18
298-102

EXECUTIVE SUMMARY

Task 1. Forward Model Simulation of the Human Electrocardiogram. Studies of sensitivity of multilead electrocardiograms (ECGs) to local ischemia/infarction were presented to the Sept. '90 International Congress of Electrocardiology. Subendocardial to transmural ischemia and infarction were simulated in each of 9 left ventricular (LV) arterial beds chosen to serve as building blocks for known variations in coronary anatomy. The smallest subendocardial area simulated in each perfusion bed was 32x4 mm (0.5% LV). This produced 50-200 μv of downsloping ST depression in 1 or more regionally specific leads, and mirror image changes in others, when scaled for distance effects from the heart to each lead. Global subendocardial ischemia (25% LV) produced 200-500 μv of ST depression in anteroapical leads. These studies led to the testable hypotheses that: (1) leads on the upper and lower left anterior torso, right anterior torso, and back are needed to optimally detect early ischemia, (2) scaling to correct for local heart-torso distance effects is needed, (3) an area of subendocardial ischemia 2-3 cm across produces significant ST changes in regionally specific leads, and (4) the lack of ST change reflects the absence of significant ischemia in spite of definite coronary obstruction.

Task 2. 16-Lead ECG During Coronary Angioplasty. Four extra electrodes supplementing the 12 simultaneous lead (12SL) ECG were placed: 1 in the left axilla, 1 on the anterior lower chest and 2 on the back. ECGs were recorded with this 16SL system in 46 patients at the time of percutaneous transluminal coronary angioplasty (PTCA). In 2/46 patients (4%) there was no chest pain, and less than 20 μv ST change on 16SL ECGs (the 98% limits of reproducibility in repeat baseline tracings); they were excluded from tabulation as negative for ischemia. In the 44 remaining patients 4 had PTCA occlusion of 2 different arteries for a total of 48 PTCAs. The ST amplitudes were scaled by the local transfer coefficients from the heart to each lead. The peak amplitude of injury current was seen in 1 of the 4 extra leads in 16 (33%). The data verify model predictions and support the hypothesis that significant additional sensitivity to ischemic change is likely with more ECG leads. From a review of the data, the 16 lead system appears suboptimal. Our multilead simulation studies, and discriminant function analysis of body surface maps by Kornreich and coworkers, suggest that 10-15 extra leads are likely to be optimal.

Task 3. 30SL Hi-Fidelity ECG Data Acquisition and Lead Locator Systems. The 3 systems described in detail in this report are performing appropriately to meet the project's scientific goals. We are acquiring Hi-Fi 30SL ECG data during exercise testing and angioplasty at the Long Beach Memorial Heart Institute. Early in the 2nd part of the follow on contract (29 May - 30 Sept. '91), when the systems are operating smoothly, we expect to install a system at USAFSAM* at Brooks AFB and directly test the model hypotheses. Those asymptomatic pilots with angiographically normal and abnormal coronary arteries, will be the target populations for adjusting the criteria to deliver optimal performance to meet the objective of detecting asymptomatic coronary disease at rest and with exercise. From the evidence just summarized in Tasks 1 and 2, screening of aircrews with the Hi-Fi 30SL ECG is expected to result in a major improvement in the detection of asymptomatic coronary disease. During this time we will continue to accumulate Hi-Fi 30SL ECG data at the Memorial Heart Institute during exercise testing and PTCA. From these two databases we expect to have enough data by 15 Sept. '91 to be able to specify explicitly the resolution, sensitivity, and specificity of the 30SL ECG in the aircrew population.

*Redesignated Armstrong Laboratory.

A-1

TABLE OF CONTENTS

LIST OF FIGURES

Figure No.

LIST OF TABLES

Table No.

OPTIMAL ECG ELECTRODE SITES AND CRITERIA FOR DETECTION OF ASYMPTOMATIC CORONARY ARTERY DISEASE--UPDATE 1990: MULTILEAD ECG CHANGES AT REST, WITH EXERCISE, AND WITH CORONARY ANGIOPLASTY

OVERVIEW AND OBJECTIVES
(Clinical Perspective--Memorial Heart Institute)

Model Building

Historically, scientific models have been used to explain inherently complex natural systems. In biology, specifically in electrocardiography and electrophysiology, Einthoven viewed the heart as a single fixed locus dipole. He used an equilateral triangle as a model of the human torso to relate the electrocardiographic signals from the 3 standard limb leads (1). For the past 80 years this model, in spite of its obvious simplifications, has formed the common basis by which clinical electrocardiographers define a "Mean Electrical Axis" for the electrocardiogram (ECG). This basis depends on both the equivalent dipole model of the heart as a current source and the equilateral triangle, or hexagonal reference system, as a model of the complex, inhomogeneous volume conductor through which these currents flow. Sir Thomas Lewis, using Einthoven's string galvanometer (2), developed the dipole layer model to explain the propagating wave of electrical excitation he found on the epicardium. This early model of excitation was extended by Allen Scher and Durrer et al. Their classic studies on intramural excitation used small, intramural plunge electrodes in animals and reperfused normal human hearts (3-6).

In developing the computer simulation of excitation of the human ventricle, we decided to build the simulation using measured anatomy, resistivities, and electrophysiology. The dipole layer model of the active electromotive surface was found to be inconsistent with measured data (7), and a new macroscopically distributed dipole model of the propagating wave front was developed from the measured intramural data. With a fine grid (1 mm^3) digital computer simulation of depolarization (QRS changes) of the human heart, we found that small myocardial infarcts, no larger than 1-1.5 cm in diameter and 0.4-0.5 cm thick, routinely produced detectable changes in the simulated ECGs (8-9). In clinical studies (10) we confirmed that clinically "silent" infarcts can be routinely detected from QRS changes in high-gain, high-fidelity resting electrocardiograms and vectorcardiograms (VCGs) when prior tracings are available for comparison. We found that serial change, or lack of it, in these ECG/VCGs is predictive of serial coronary and ventriculographic change, or lack of it, with 98% accuracy. This finding is particularly relevant to the pilot population in whom, for reasons discussed in the Air Force perspective later, we can assume that more than half of the myocardial infarcts suffered will have been clinically unrecognized, or "silent."

Harumi, Burgess, and Abildskov were the first investigators to develop a model of the T wave (11). Thiry and Rosenberg later developed a 3-dimensional simulation of repolarization (12). Miller and Geselowitz developed a 4 mm^3

grid heart model in a homogeneous torso in which they manually entered changes in excitation and recovery parameters (13,14). Essentially, over the past 5 years, we have been automating the grid heart model of Miller and Geselowitz using a 1 mm^3 grid heart in an inhomogeneous torso. The success of these models in simulating typical 12-lead ECG changes of ischemia, injury, and infarction, by incorporating action potential waveshapes and distributions typical of those measured in the laboratory, makes the likelihood of success with the fine grid version quite high.

THE SELVESTER-SOLOMON MODEL AND THE 30 LEAD HI-FI DATA ACQUISITION SYSTEM (Relevance and Significance to the United States Air Force [USAF])

Ten to 20% of all apparently healthy people over 35 years of age have significant but undiagnosed coronary artery disease. For about 25% of these people sudden death is the first symptom of heart disease and as many as half of those who die have had a prior unrecognized infarct (heart attack). Applying these statistics to USAF pilots, at least 1 pilot per 10,000 over the age of 35 who fly an annual average of 300 h in high-performance aircraft will die suddenly each year at the controls, resulting in the loss of life and aircraft. Based on published reports, the total cost of replacing such lost aircraft is between 30 and 50 million dollars annually. Furthermore, it follows that there are 10-15 unrecognized new infarcts per year for every 10,000 of these flyers. Improving the identification of coronary artery disease in these pilots would lower the number flying with unrecognized heart disease. This identification would decrease the chances of sudden death of pilots at the controls, and reduce the number of aircraft lost. The identification of even 1 in 10 pilots of high-performance aircraft with totally unsuspected coronary disease would be expected to save the government $3-5 million per year by preventing loss of aircraft and pilot. From our previously reported findings, and from the multilead ECG recording with the Case 12 system summarized in this report, there can be little doubt that the routine screening of apparently healthy aircrews with Hi-Fi Signal Processed 30 Simultaneous Lead (30SL) ECG recordings during rest and exercise will significantly improve the detection of asymptomatic coronary disease. We have documented in earlier studies (10) that serially recorded 30SL ECGs should allow us to detect new "silent" infarcts with 98% confidence. We expect these techniques to detect significantly more than 1 in 10 pilots each year with coronary artery disease that are not now being identified.

The task for the current ongoing contract year is to define the optimal lead number, location, and criteria in these leads, and to define the limits of resolution for the detection of "silent" ischemia. Along with this information the sensitivity, specificity, and predictive accuracy of this technique would also be accomplished. With this information it will be possible to accurately define the cost-effective trade-offs for the implementation of such a screening process in the USAF medical system worldwide. The ultimate goal of this effort is the development of a portable ECG Mapping Cart that can be used in flight surgeons' offices for resting and exercise ECGs to improve "silent" coronary artery disease detection in asymptomatical aircrews.

OVERVIEW AND OBJECTIVES
(U.S. Air Force Perspective)

Gil D. Tolan, Colonel, USAF, MC

(Authors note: this summary from an earlier statement of work is presented here because it gives those from outside the Air Force, including our consultants, a perspective from "inside" that would not otherwise be available).

Although coronary artery disease mortality in the United States decreased 22.6% between 1969 and 1977, at 670 deaths per 100,000 men per year, coronary artery disease still remains the number one cause of death in this country. Coronary artery disease is the cause of 70% of the nontraumatic deaths in the active duty U.S. Air Force. Rated flying personnel are not immune to developing coronary artery disease. Each year approximately 50 rated pilots and navigators on flying status are admitted to USAF hospitals where the discharge diagnosis is coronary artery disease (ICDA codes 410 through 414). Each year approximately 8 rated personnel on flying status suffer fatal myocardial infarctions. It is hard to say how many USAF aircraft accidents per year are due to coronary artery disease because frequently there is no heart found to autopsy after the crash, and because the on-board recorder does not record the ECG. Even if a pilot suffered an acute myocardial infarction in flight, there would not be sufficient time between that event and when the rest of the heart died in the crash to distinguish the acute infarction. It takes hours to days for the necrosis of an infarction to become evident at autopsy. The Armed Forces Institute of Pathology has a policy of not attributing an aircraft crash to coronary artery disease merely because an old myocardial infarction scar is found or because coronary atherosclerosis is present. Today 44% of the rated force is over 35, the age susceptible for coronary artery disease. Coronary artery disease is not confined to just older pilots. Autopsy studies on military men killed in combat in both Viet Nam and Korea found coronary artery disease in many young troops. Although we do not know how many aircraft accidents per year are due to coronary artery disease, we do know that approximately six times per year a USAF aircraft for no apparent reason impacts the ground with no prior communication from the pilot and no attempt to eject. Some suspect that the pilot was trying to recover an out of control aircraft right up to the end, but others believe the lack of any communication of trouble implies sudden human incapacitation. Although there are many causes of sudden incapacitation, common things occur commonly, and coronary artery disease is the most common cause of sudden incapacitation in American males.

Today the screening for coronary artery disease in the USAF rated force relies solely on the standard 12-lead ECG. The Framingham 14-year followup of 5,000 men and women considered free of heart disease at onset found that the standard 12-lead ECG was normal in 2 out of every 3 cases which suffered a myocardial infarction in the subsequent two years. This represents a 33% sensitivity for the standard 12-lead ECG as a predictor of a myocardial infarction in the next two years. The Framingham study also found that in those cases with scars from old myocardial infarctions found at autopsy, 36% of

these were unrecognized during life by both the patient and his doctor. In 16% of all coronary cases, the first symptom was sudden death.

Most USAF flyers enjoy flying, they get paid extra to be on flying status, and often their career progression requires that they be fit to fly. Although most flyers have IQ's three standard deviations above the mean, they nearly all score three standard deviations above the mean on the MMPI denial scale. Their ability to deny risk is a life preserving attribute that prevents them from panicking when exposed to enemy fire. These same factors, however, decrease a flyer's propensity to report his chest pain to his flight surgeon.

In the new generation high-performance aircraft, flyers are frequently exposed to greater than 7 +G forces. By the end of this decade (the 1980s), two-thirds of USAF active duty pilots will be flying high-performance aircraft. These aircraft place unprecedented demands on the heart to keep the brain perfused. Within 30 seconds of pulling 7 +G's, the pooling of blood in the lower lobes of the lungs causes the alveolae to collapse, creating a ventilation perfusion abnormality such that in healthy nonsmokers their mean arterial oxygen tension drops from 91 to 46 mmHg. At the very time the demand for cardiac output is maximum, the oxygen supply to the heart is being decreased by both this ventilation perfusion abnormality and by the shortening of diastolic filling time from the faster heart rate. Since flow of a liquid through a tube is inversely proportional to the fourth power of the radius, a slight decrease in a coronary artery's diameter can have a big effect on the amount of blood that gets by that obstruction should the flow remain laminar. Because a slight obstruction can cause turbulance, a slight coronary obstruction can be more hemodynamically significant than implied by the percent diameter narrowing. Furthermore, a healthy coronary artery can increase flow ninefold by dilating during peak workloads. By preventing dilation, circumferential atherosclerosis, even if minimal on angiography, can profoundly reduce myocardial oxygen supply during peak loads. Even without causing a myocardial infarction, an asymptomatic coronary narrowing can decrease maximum cardiac output during sustained high +G maneuvers. If during a high +G maneuver the pilot's brain is not perfused, then under the best of circumstances, it will take him on the average 15 seconds to recover from his loss of consciousness. By then it may be too late to recover his supersonic aircraft. Thus, a slight coronary artery narrowing which might never cause an infarction on the ground could prove fatal under the sustained high +G profiles of the new generation aircraft.

For all the reasons just cited, flying safety requires that we not wait for the flyers to come to their flight surgeon complaining of chest pain to begin worrying whether they have coronary artery disease. We need to be able to detect coronary artery disease while it is still asymptomatic. At this time the National Institutes of Health have no plans to fund research into detecting asymptomatic coronary artery disease because "the only treatment for it is advice to modify risk factors and that advice should be given regardless of whether coronary artery obstructions already exist." If medical technology is to keep pace with the demands of new aircraft technology, then it is up to the USAF to develop a better system to detect coronary artery disease.

The goal of this contract is to develop a system which is better than the existing method at distinguishing rated flyers with aeromedically disqualifying coronary artery disease from healthy flyers. This includes detecting both coronary artery obstructions (ischemia) and myocardial infarctions (scars). Correctly localizing infarctions and coronary obstructions with a screening test in the field is not a requirement of this contract.

Good skin-to-electrode contact is essential to accurate electrocardiography, but good contact during stress testing is difficult to maintain because the adhesive may loosen as the patient moves and perspires. The more electrodes one adds, the greater this problem. Furthermore, additional electrodes require additional time to apply, more channels for recording and more complex analysis, all of which increase the cost. For these reasons, the USAF needs to use enough electrodes in both resting and stress electrocardiography to ensure flying safety without adding any extra electrodes merely to determine some day if they might be useful. Any addition of electrodes will incur a considerable expense not only to acquire new ECG carts for the field, but also to train USAF physicians to interpret the new leads. For this reason, any new lead must be based upon strong scientific evidence that it adds important information not currently available. Because the expense and risks of both false positive and false negative errors are considerable, the process in developing such scientific evidence must be meticulous in every detail. Because current policy requires that rated flyers with abnormal stress tests be grounded until proven healthy by cardiac catheterization, it is essential that any new screening system maintain a specificity of 95% or better.

In 1974, Victor Froelicher, Jr., Maj, USAF, MC, reported in the American Journal of Cardiology on a group of 1,390 asymptomatic men screened at the USAF School of Aerospace Medicine for latent coronary artery disease with a double Master's two-step test followed by a symptom-limited treadmill exercise tolerance test. The follow-up period ranged from 4.1 to 8.4 years (mean 6.3). End points for coronary artery disease were angina pectoris, acute myocardial infarction and sudden death. Only lead X (CC5) was always recorded during exercise. Leads II, III, aVF, V2 and V5 were recorded before exercise and during recovery. In this follow-up study, the Master's test had a sensitivity of 61% and a specificity of 92%. Subsequently, this institution has recorded four leads (X, Y, Z, and CM5) during all phases of the treadmill test. No follow-up study of this lead system has been done, but we know that 60% of the asymptomatic flyers with abnormal ST segment depression of symptom-limited stress testing have no coronary artery disease found on cardiac catheterization with left ventriculography and selective coronary angiography. We have also found advanced coronary artery disease in three dozen asymptomatic flyers with normal or only borderline abnormal ST depression on their treadmill test.

In a series of four articles published in Circulation in 1973 and 1974, Fred Kornreich, M.D., of the Free University of Brussels, pointed out that neither the Frank lead vectorcardiogram nor the standard 12-lead electrocardiogram contain all the information projected by the heart to the body surface. Dr. Kornreich found that with 24 leads and a single transformation formula for all body types, one could closely reconstruct a complete body surface map. Subsequently, Robert Lux, Ph.D., at the University of Utah, Roger Barr, Ph.D., at Duke University, and others have shown that a least 24

electrodes are needed to capture all the information projected by the heart to the body surface. What remains to be determined is whether 24 electrodes are necessary to detect all disqualifying asymptomatic coronary artery disease in the USAF rated force. In 1980, Dr. Kornreich reported at the Engineering Foundation Conference on Computerized Interpretations of the ECG that adding just four electrodes to the standard 12-lead ECG for a total of 16 leads significantly improved the sensitivity and specificity of bonafide myocardial infarctions over just the standard 12-lead ECG or just the Frank lead VCG. At the same meeting, Frank Yanowitz, M.D., of the University of Utah, reported that using 32 leads doubled the sensitivity of stress tests for cardiac catheterization-proven significant coronary artery disease compared to using the standard 12-lead system for stress testing. He also suggested that not all 32 leads were necessary, but needed more data to prove this. In 1980, at the Computers in Cardiology Conference, R. von Essen of the Helmholtz Institute for Biomedical Engineering in West Germany, reported that a 48 precordial lead stress test had a 96% sensitivity and 95% specificity compared with 56% sensitivity and 95% specificity of the 12-lead system for stress testing. Other investigators have reported similar improvements in sensitivity while maintaining 95% specificity by doing surface potential mapping with stress testing.

NOMENCLATURE OF REGIONAL LEFT VENTRICULAR SEGMENTS

Considerable ambiguity exists in the current literature about the nomenclature and definition of the regional or segmental anatomy of the heart. Throughout this document we will be using the left ventricular (LV) segmental subdivision nomenclature shown in Figure 1. This subdivision is a modification of the Ideker subdivision reported in a number of recent papers (17-20). These octant circumferential subdivisions of the LV are combined by twos into quadrants (see lower right illustration in Fig. 1). The LV is further subdivided from apex to base by passing 2 planes through it at right angles to the long axis of the LV. Careful placement of these planes allows for the division of the internal long axis into equal thirds. This system produces a 12-segment subdivision of 4 walls (anteroseptal, anterosuperior, posterolateral, and inferior) with 3 subdivisions each (basal, middle, and apical) as shown in Figure 1.

SEGMENT SUBDIVISION

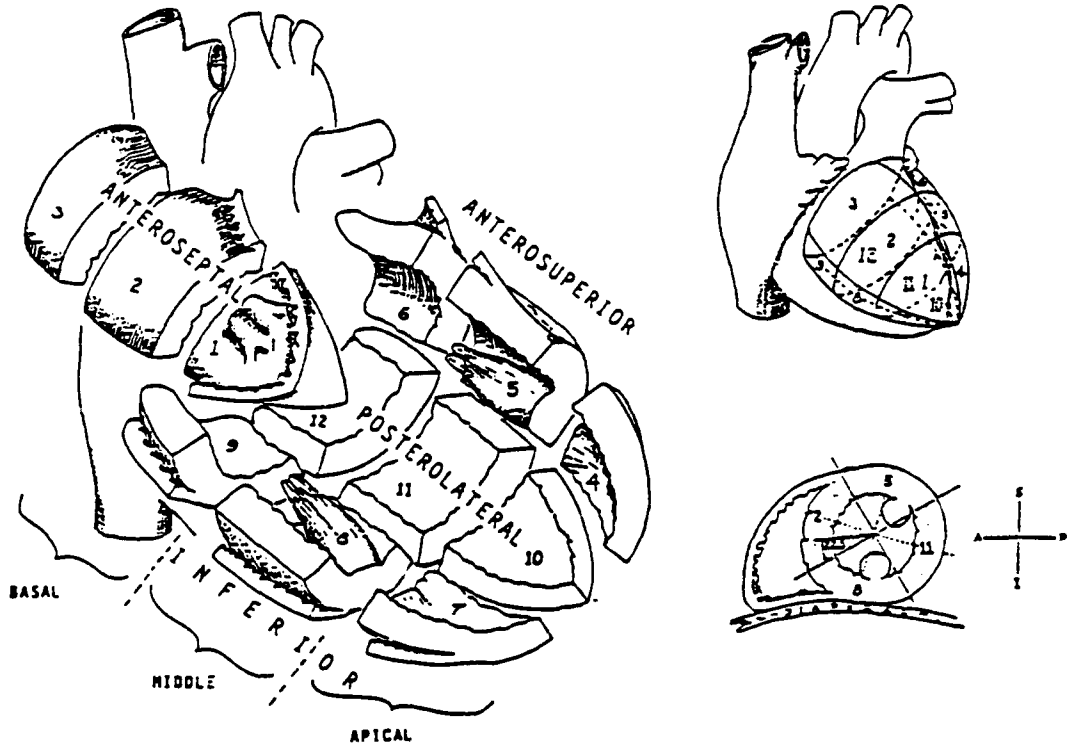

Figure 1. Twelve-segment left ventricular (LV) subdivision and nomenclature. The advantage of using this specific subdivision is that it divides the LV into segments that are in close approximation to the usual blood supply to each of the regions, i.e., segments 1-7, and 10 by the left anterior descending coronary, 8 and 9 by the right, and 11 and 12 by the circumflex.

OPTIMAL ECG ELECTRODE SITES AND CRITERIA FOR DETECTION OF ASYMPTOMATIC CORONARY ARTERY DISEASE--UPDATE 1990: MULTILEAD ECG CHANGES AT REST, WITH EXERCISE, AND WITH CORONARY ANGIOPLASTY

INTRODUCTION AND BACKGROUND

The computer simulation of the total body surface human ECG developed by us over the past several years was constructed from measured cardiac and torso anatomy, resistivities, and electrophysiology (8,9,15). Bipolar cardiac intramural plunge electrode data was used to develop a model of the active electromotive surface (16). By the method of Huygens, the propagation wave of excitation was simulated in the normal human heart discretized at a 1 mm^3 resolution (17) and projected to some 1,300 sites on a realistic inhomogeneous torso that includes intracardiac blood mass and lungs. All reasonable combinations of intraventricular conduction defects, ventricular hypertrophies, and myocardial infarcts of all sizes in any feasible location (9) were simulated. QRS criteria for infarct size resulting from these numerical experiments (18,19) have been validated in a series of classic pathoanatomic studies (20-24) and summarized in a USAF School of Aerospace Medicine Technical Report (31).

The model has since been enhanced (25)(as proposed in the Technical Report) to include the simulation of the human myocardial repolarization process and the STT portion of the ECG, which is most sensitive to myocardial ischemia. The basic models of Harumi, Burgess and Abildskov (11), Thiry and Rosenberg (12), and Miller and Geselowitz (13,14) were adapted and upgraded by incorporating individual action potential waveforms into each 1 mm^3 "cell" of the comprehensive fine grid model. These local action potentials were modified to emulate the changes observed during ischemia. Simulations of regional subendocardial ischemia produced ECG changes typical of those seen in these conditions. This information led to the publication (26) of a recommended lead set of 20 simultaneous leads (20SL) and testable ECG criteria for the detection (and quantitation) of ischemia in any coronary artery distribution. Task 1 of this report includes details of more recent numerical experiments with the "Forward Model" simulation that speak more directly to the sensitivity and probable resolution of the method. During this same period, Kornreich and associates were continuing to report discriminant function analysis of 150 lead body surface maps for the optimal lead location and ECG criteria to discriminate multilead ECGs of normals from those of patients with LV hypertrophy, anterior infarct, inferior infarct, and non-Q infarct (27-29). Optimal discrimination of these entities required leads in the upper and lower left anterior torso, right anterior torso, and on the back. The 30SL system proposed represents an ongoing collaborative effort between the European and Canadian workers in the field and ourselves.

Besides the 2 reported studies with the model just described, 2 additional related studies have been done during the period since the 1985 Technical Report. The first was a multicenter study of the short-term effects of carbon

monoxide exposure in an environmentally controlled chamber (30). On each of 4 test days 63 men with documented coronary disease and effort angina performed 2 symptom limited treadmill tests for a total of 8 tests each. The tests were separated by a recovery period and 50-70 min. of random exposure to either room air or air containing 1 of 2 concentrations of carbon monoxide. The subjects and the testing personnel were blinded to the exposure. All subjects had 12SL signal averaged, median beat ECGs recorded during exercise. This data gave us firsthand experience at the Rancho Los Amigos Medical Center acquiring hi-fidelity (Hi-Fi) 1 ms digital ECG data during exercise testing and signal processing this data.

The second related study during this period was done with Myrvin Ellestad's group at the Memorial Heart Institute of Long Beach. The Marquette Case 12 system, with 4 extra precordial leads added to the 12SL system was used. This resulted in a 16SL ECG system. In Task 2 of this report we will describe the results of recording 16SL ECG data with this system during percutaneous transluminal coronary angioplasty (PTCA) in 46 patients with documented coronary disease. The 4 extra leads of this system were added on the left upper and lower thorax and on the back of the patients. The 16 lead set is most likely a suboptimal set. The set represented an interim solution allowing us to continue work on the basic project while we sought funds for a more appropriate 30 lead system. Work with the model simulations and the findings of Kornreich and associates had suggested that greater sensitivity and specificity to regional ischemic change were to be expected with perhaps up to 10-15 leads added to the standard 12SL ECG. The data derived from the 16SL preliminary study can be assumed to be one more building block in defining the ideal number and location of ECG leads for the optimal detection of asymptomatic coronary artery disease. The technical details, including the 30SL ECG Hi-Fi. digital data systems and the lead locator systems, are described in Task 3 of this report.

TASK 1: FORWARD MODEL SIMULATION OF THE HUMAN ECG

Multilead ECG Criteria for Detecting Regional Ischemia

METHODS

The fine grid Selvester-Solomon model of depolarization-repolarization (QRS-T) of a digitized human heart imbedded in a realistic inhomogeneous male torso, which included intracardiac blood mass and lungs (25,26), was modified to simulate local regions of ischemia as follows: The repolarization generators were constructed making use of an equation containing 3 arbitrary parameters that assume values which permit the time course of the myocardial action potentials to be approximated (refer to appendix of reference 31 for details). The 3 parameters characterizing the action potentials are the recovery potential, rate of repolarization, and the functional refractory period. With these 3 parameters and 4 constants (initial resting potential, time to depolarize, peak depolarization potential, and a time constant which represents the time for the local region to reach equilibrium), each discrete point within the myocardium can be represented by a unique waveform (Fig. 2). These

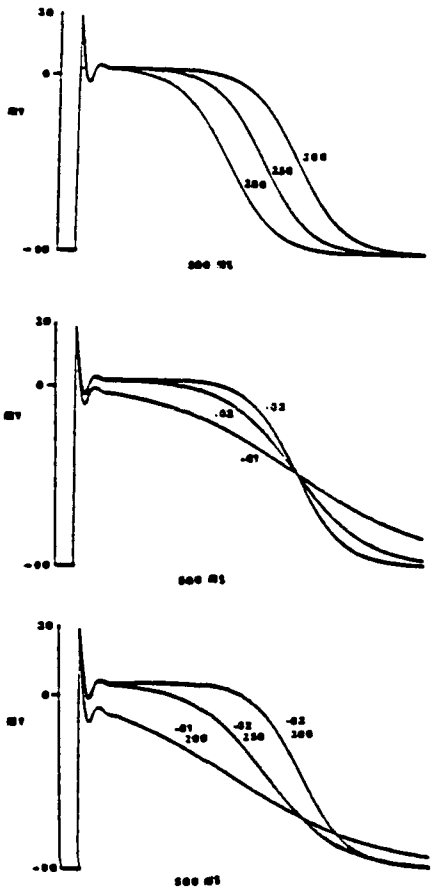

Figure 2. Action potential waveforms generated by the model. In the top set of waveforms, the functional refractory time (phase 3) was changed. In the middle set of the waveforms slope of phase 3 was varied. In the bottom panel, the functional refractory time and the slope were varied as shown.

parameters are found by a table look-up that incorporates the endocardial to epicardial gradient in action potential duration and refractory periods as well as the apex to base gradient. A separate table contains the 4 constants just described that are mainly influenced by injury, ischemia, and the electrolyte milieu of the active cells. The individual waveforms from each cubic millimeter "cell" were then projected to 20 regional cardiac generators and combined with a Gelernter-Swihart solution for the heart-to-chest transfer impedances as described previously (15, 25, 26, 31). A copy of reference 26 is given as the appendix. Combining the generator and transfer impedances yielded a mathematical-physical simulation containing the action potential parameters that were adjusted within the known electrophysiological variability so that computed QRS-T were made to agree with normal vectorcardiograms and 12-lead ECGs. This model now allows for the specification of local areas of injury, ischemia, or infarction by their effects on the local myocardial action potentials.

The specific geometry of local areas of subendocardial ischemia in each of the major coronary artery distributions was specified using the propagation forward model. A start point for the propagation was chosen near the center of the endocardial surface of the segment in which subendocardial ischemia was to be simulated. The model was then run with a 4-to-1 Purkinje to myocardium propagation velocity. Four consecutive time steps (10 ms.) resulted in a defined domed volume 32 mm in diameter at its base on the endocardium and projecting 4 mm into the subendocardium at its center, as shown in Figure 3. The program saves the coordinates of these points. The individual action potentials of each of these 1 mm^3 "cells" can now be altered to represent various degrees of injury, ischemia, or infarction. In the example shown in Figure 3, subendocardial ischemia in this volume was simulated by reducing the resting potential, the functional refractory period, and the downslope by 50% each. The effects of various degrees of ischemia, from mild to infarction, in these small subendocardial regions, and larger ones extending to the mural and transmural myocardium, was systematically explored with the simulation.

Ischemia involving the entire subendocardium of each of 10 coronary arterial perfusion beds shown in Figure 4 was simulated by choosing the start points so that at the end of the 4th time step the boundary of the designated volume would represent that of the particular coronary bed. By selecting a slower Purkinje propagation velocity, more of the subendocardium is included near the boundary of the ischemic region. The 10 arterial distributions shown in Figure 4 were chosen to serve as building blocks. Various combinations of these modules can be made to represent regional ventricular segments with a variable blood supply. In this way, variations seen in coronary blood supply, such as right dominant, left dominant, balanced, and variations in the distribution of the main branch arteries (diagonals, ramus intermedius, and circumflex marginals, etc.) can be accommodated.

The systematic exploration of effects of various degrees of ischemia in each of the coronary distributions led to the publication (26) of a recommended lead set of 20 ECG lead locations and a testable set of criteria for diagnosis and quantitation of ischemia in the 12 segment LV subdivision. This publication, those by Kornreich (27-29), and wide-ranging discussions with various Canadian, European, and United States mapping groups, has led to an attempt to establish a limited lead set of 24, 30, and 32 leads which are subsets of the 150 and more leads used by the various body surface mapping groups. There is a consensus that any expanded lead set should include the standard 12-lead ECG, the Mason-Likar 12-lead ECG, and the Frank orthogonal 3-lead set as a minimum. The 30SL lead array shown in Figure 5 represents the present status of that effort, and includes the Grishman Cube and the McFee orthogonal lead locations as well. We expect the Kornreich discriminant function, the Lux orthonormal basis function, and the Horan-Flowers multipole expansion transformations to each be assessed with the final consensus version of this lead set.

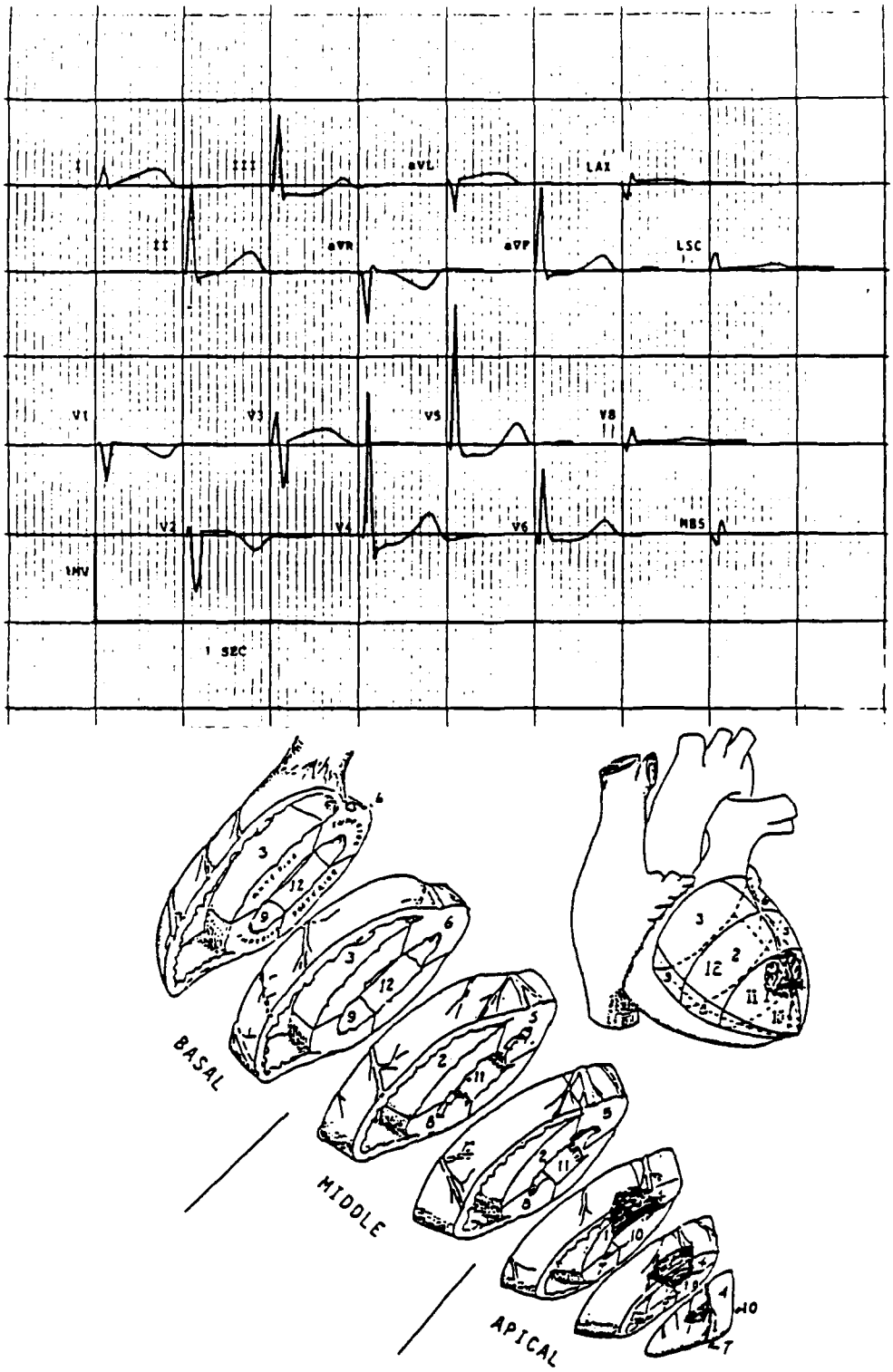

Figure 3. A simulated small subendocardial ischemic zone localized in the anteroapical area of the LV. The ischemic region measures 32 mm in diameter and extends 4 mm in from the endocardium (representing 0.5% LV). The 16SL ECG from this simulation is shown in the top panel.

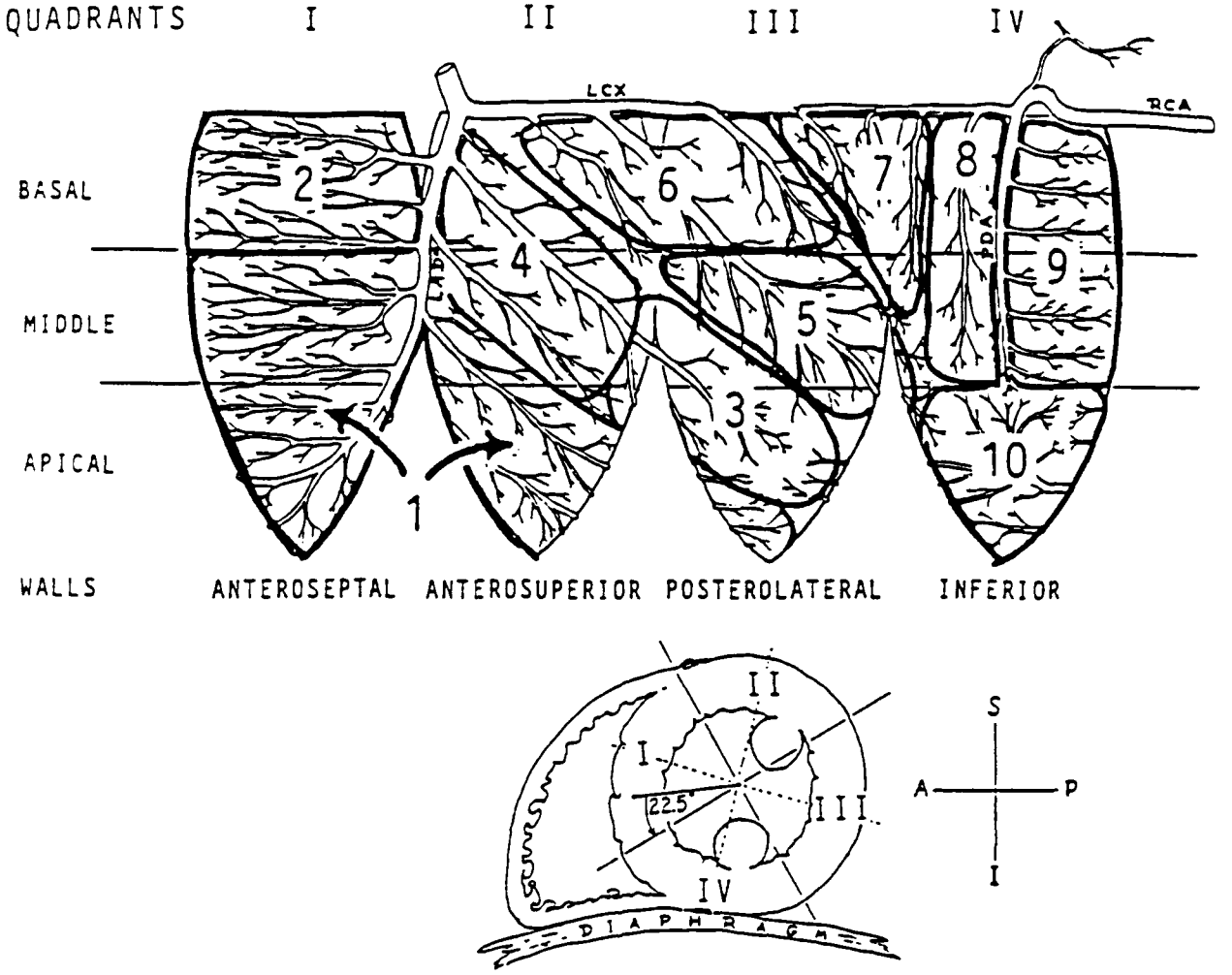

Figure 4. A Mercator projection of the epicardial surface of the LV with the distribution of 10 arterial subdivisions used as building blocks in the model for various coronary distributions. This specific circumferential quadrant subdivision, as indicated in the cross section of the heart above, has the advantage of dividing the septum along the lines of the perfusion beds of the septal perforator branches of the left anterior descending (LAD) and the posterior descending artery (PDA) branch of the right coronary artery (RCA). The antero-septal wall is perfused by the LAD which also typically supplies the anterosuperior wall and most of the 4 apical segments. The base of the anterosuperior wall has a dual blood supply from diagonal branches of the LAD and marginal branches of the left circumflex (LCX). The posterolateral wall, except for the apical segment is usually supplied by the LCX artery and the inferior wall by the RCA (through its PDA and distal inferior wall branches). The inferior portion of the septum, perfused by the PDA is included in the inferior wall.

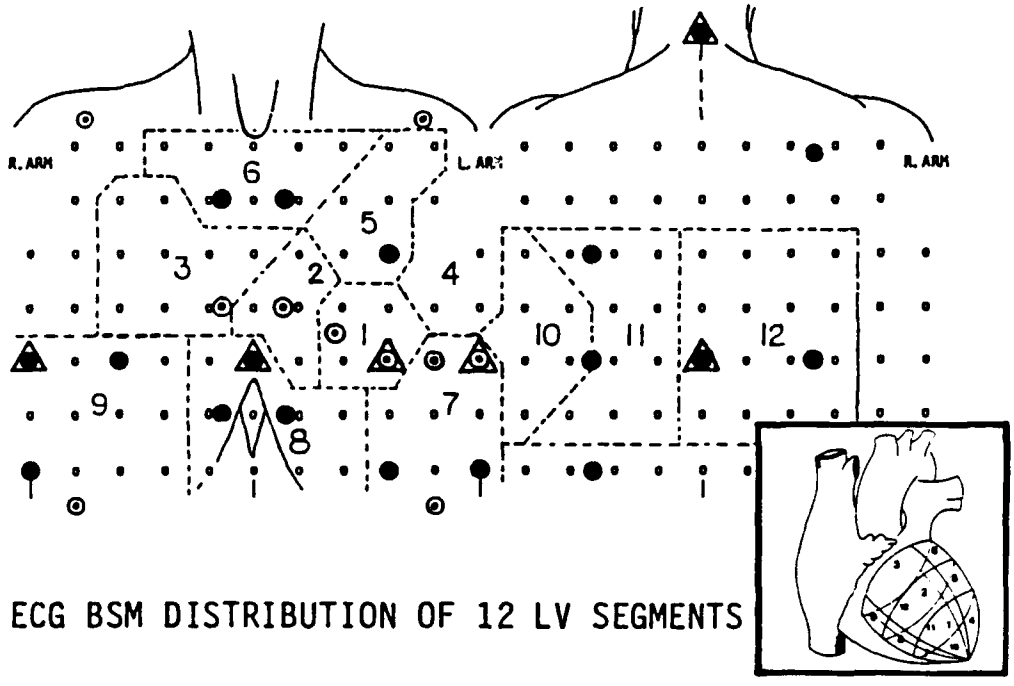

Figure 5. Lead locations for the 30SL ECG on a body surface map and the map projections of the 12 LV segments illustrated in Figure 1. The baseline supine and standing 30SL ECG is recorded first with the limb electrodes on the extremities and then with these electrodes moved to the Mason-Likar locations. The middle row is located according to the conventional A.H.A. bony landmarks for the 12-lead ECG and it's right precordial counterpart. The triangles are the specific leads of the Frank orthogonal subset. The upper and lower rows are each 10 cm above and below the middle row, except for the neck lead on the 7th cervical vertebra and the right upper back lead which is placed 20 cm above the right lower back lead (V8R).

RESULTS

Small volumes of definite subendocardial ischemia (or infarction), such as that shown in Figure 3, when simulated in each of the major coronary artery distributions consistently produced ST segment depression in the regionally specific leads previously identified when simulating infarct with the model. This volume is about 0.5% of the total LV volume. More extensive involvement of the subendocardium in each of these regions produced even more definite ST depression, shown in Figure 6, which is an example of ischemia in the subendocardium of arterial subdivisions 7 and 8 of Figure 4 that is supplied by posterior wall branches of the distal right coronary artery. The volume of ischemic myocardium in this example calculated out to be 1.5% LV. When each lead is scaled to the heart-torso lead transfer impedances of the ischemic region the ST segment depression was maximal in the region specific leads and was similar throughout for the same volume of ischemic subendocardium. Global subendocardial ischemia, as postulated by Ellestad (32), (such as that shown

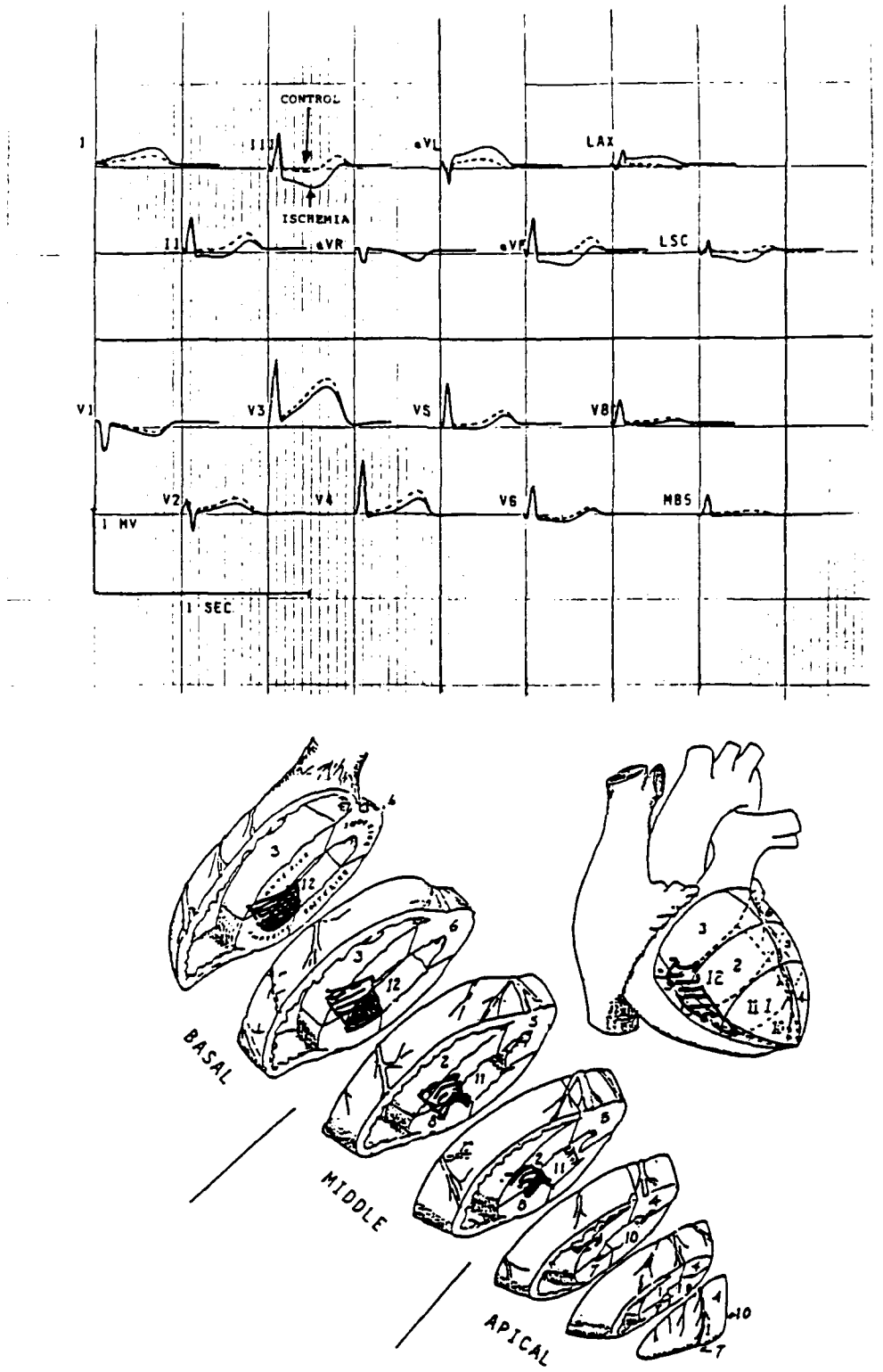

Figure 6. 16SL ECG of simulated subendocardial ischemia in the distribution of the inferior posterolateral branch of the RCA illustrated in the lower panel.

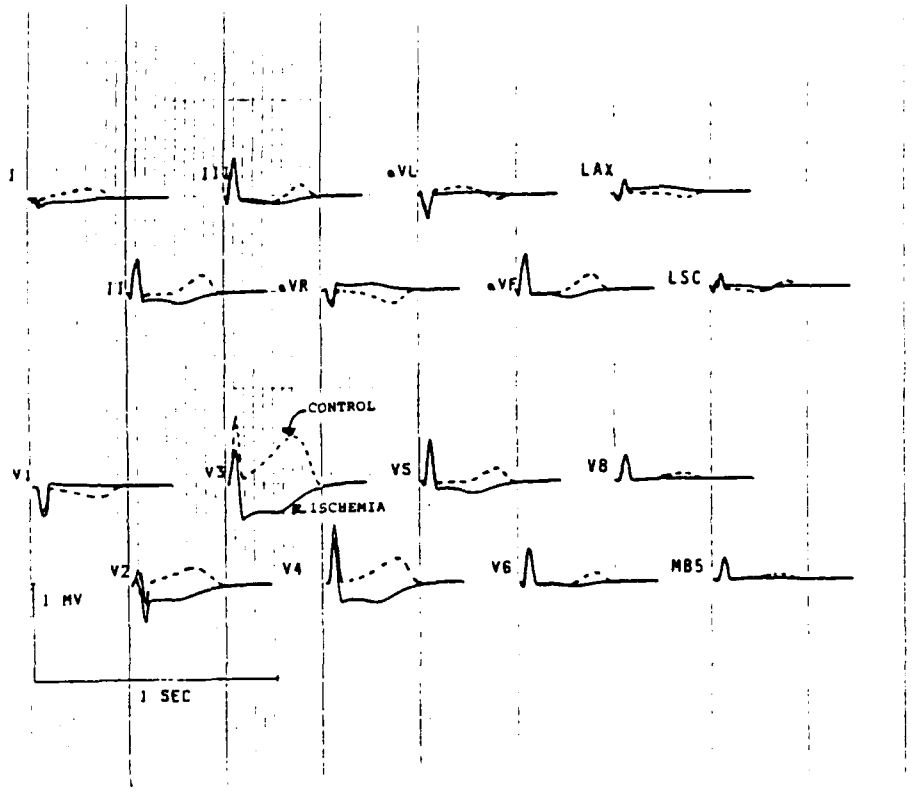

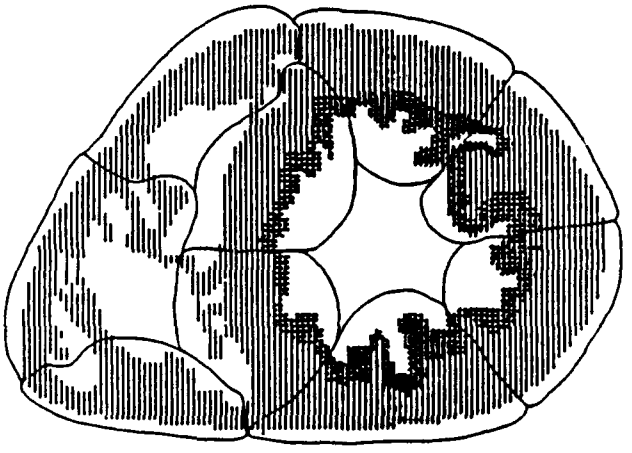

Figure 7. 16SL ECG of simulated global subendocardial ischemia involving the inner 4 mm and 25% of the LV. The lower panel is a cross-section at the 45 mm level of the heart based on the simulation. The ischemic region is indicated by the shaded endocardial area.

in Fig. 7) produces much more definite changes in anterior and apically oriented leads in spite of a great deal of internal cancellation of oppositely directed current fields located around the circumference of the LV cavity. In this case, 25% of the LV volume is ischemic.

DISCUSSION

In simulated normals and subendocardial ischemia being reported here, the depolarization current field (QRS vector) from a local myocardial region and the local repolarization field (STT vector) from the same coronary distribution are essentially parallel to each other. This observation leads to a procedure for selecting a set of ECG recording sites that include the effect of the thorax. A unit source in each of the myocardial regions is given the mean direction found in the forward model to simulate the normal QRS-STT ECG data. With the unit sources defined this way the simulation is executed separately for each unit source. This yields 1,300 body surface ECGs for each specific local region from which to choose an optimal set of recording sites. These unit source ECGs are heart-to-chest transfer impedances. The majority of the 1,300 body surface sites are about 1 cm apart. One of the advantages of selecting ECG lead recording sites this way is that we can take advantage of the proximity effects between local myocardial regions and the body surface.

One of the major strengths of a simulation that has been constructed from measured electrophysiological data and anatomy is that results of the simulations can then be related to the anatomy and electrophysiology directly. Hypotheses can be generated from these results that relate to the anatomy, electrophysiology, and current field theory, and these hypotheses can be directly tested in the clinical environment. The study of ECG changes at the time of balloon angioplasty in Task 2 of this report is one such study. The procurement and implementation of the Hi-Fi 30SL ECG data acquisition system described in Task 3 now provides the tool to test the proposed lead system, and the proposed criteria in these leads, for detecting unsuspected coronary artery disease in the asymptomatic pilot population. The interaction between the model criteria and the clinical findings with angioplasty occlusion of specific coronary arteries will be taken up in the discussion section of Task 2, and in the final conclusions and recommendations of this technical report.

CONCLUSIONS

Small volumes of subendocardial ischemia, as defined in this simulation and with this torso model, consistently produced definite changes in simulated body surface ECG leads. When myocardial action potentials of subendocardial regions representing less than 1% of the left ventricle were decreased by 50% in their resting potential, functional refractory period, and downslope of the repolarization, definite ST depression occurred in the leads shown in earlier simulations (31) to be most sensitive to that region. When the amplitude of the local ECG waveform was normalized to the transfer impedances from the local segment to the specific lead, the ST depression observed was of the same magnitude if the same degree and volume of ischemia was simulated in any regional coronary perfusion bed. In this simulation, additional ECG leads are needed on the right anterior torso, upper and lower left anterior torso, left flank, and on the back (as shown in Fig. 5) for maximum sensitivity to these local ischemic regions. It is now imperative to validate these lead locations, and criteria in these leads, in carefully controlled studies in subjects with and without documented coronary disease. Multilead ECG recording during exercise stress testing in a population of patients being worked up for probable coronary disease with perfusion scans, wall motion studies with exercise, and with coronary angiography are needed to define the sensitivity and resolution of the method. Similar recordings in a significant population of documented normal subjects will also be needed and displayed as receiver operator curves to optimize the sensitivity and specificity.

TASK 2: 16-LEAD ECG RECORDING DURING CORONARY ANGIOPLASTY

METHODS

The study population consisted of 46 patients who had undergone elective percutaneous transluminal coronary angioplasty (PTCA) as a part of their regular cardiology care at the Long Beach Memorial Heart Institute during the years 1987-1989. There were 35 men aged 40-80, mean 59.5 yr, and 11 women aged 49-75, mean 64 yr. Each patient and the attending cardiologist had agreed with informed consent to having the 16-lead ECG recording done before and during the PTCA procedure. The recording was done with a commercially available system (the Marquette Case 12) using a version with 4 extra leads added to their standard 12SL ECG recorder. The 12SL ECG is made up of 2 independent limb leads, from which the other 4 are computed, and 6 independent precordial leads for a total of 8 independent leads. Thus, when the 4 extra leads are included in the set as precordial leads there are 12 independent simultaneous leads which, when combined with the 4 computed ones, make up the 16SL ECG system. The system generates hard copy of the 16 leads on demand or in a preset protocol in 10 s episodes with a signal averaged median beat. The system stores this data in magnetic form which can be downloaded on 3-1/2 in. diskettes for later replay through the system. The amplitude of the ST segment at an arbitrarily chosen interval after the J point is also routinely printed out with the waveforms for each episode, and plotted as a trend plot or a series of them at the end of each recording session. In this study the ST 70 point used in routine exercise testing at the Memorial Heart Institute was chosen for all studies.

After careful skin preparation with acetone/alcohol and vigorous scrubbing, radiolucent electrodes were placed in the lead locations shown in Figure 8. Baseline recordings were initially done with the limb leads on the extremities. These leads were then moved to the modified Mason-Likar locations (33) shown in the figure. The 4 extra electrodes were placed as follows: LAX in the left axilla, LSC in the left subcostal margin at the level of AVF (7th intercostal space in the mid clavicular line), V8 on the back (opposite V4) and MB5 in the midback (both the latter at the level of V4-V6). Recordings were made in the angio suite as the patient was being prepared, before any intervention and at each stage in the procedures (i.e., before and after angiograms, catheter and wire insertions, etc). The ECG was monitored throughout the procedure. A set of recordings was made under the systems program control every 15 s during each occlusion with the angioplasty balloon, and until the ECG was deemed visually stable post occlusion. At a later date all tracings were reviewed by 2 independent experienced readers verifying the onset-offset of waveforms and J point chosen by the algorithm. Any differences were resolved by consensus with a third reader. Any tracing with unusually noisy data or motion artifact was disregarded which, in general, was an uncommon occurrence. The data quality was considered excellent when the raw data was compared to the median beat generated at each 10 s epoch.

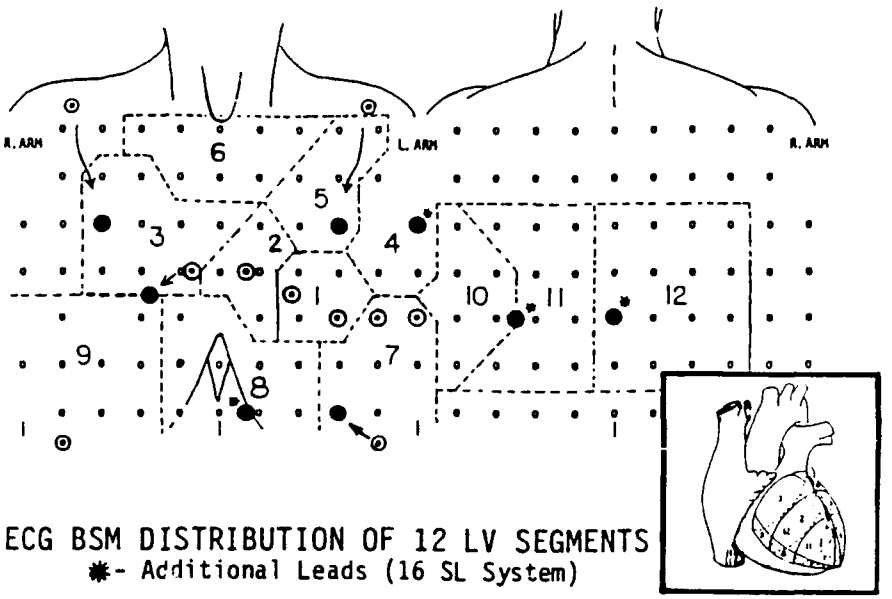

Figure 8. The 16SL ECG lead locations on a body surface map that were used in the angioplasty study. The Mason-Likar lead locations were modified by moving the left and right arm electrodes to the upper torso at the level of the third interspace in the respective mid-clavicular lines. AVF was located at the left lower costal margin directly below V4. The 4 additional electrodes shown by the * are: LAX, left axilla; LSC, left subcostal margin at the level of AVF; V8, on the back (opposite V4); and MB5, midback at the same level.

One patient developed angina and classic ischemic ST depression with wire insertion past a tight obstruction in the proximal left anterior descending. The angina did not completely resolve with vasodilators in spite of evidence of contrast flow past the lesion around the guide wire. After a number of unsuccessful attempts to pass a balloon catheter past the lesion, the procedure was abandoned and the patient sent for urgent bypass surgery. Since the patient did not have documented complete occlusion with the balloon catheter, the patient was not included in the tabulation results and will be discussed separately. Two additional patients with PTCA occlusion of the right coronary artery (RCA) developed no chest pain and exhibited no STT change during several sequential balloon occlusions of this artery. Since our goal was to test the ability of the multilead ECG to localize ischemic currents of injury when they occurred, and there were no documented signs or symptoms of ischemia, these 2 patients were excluded from the tabulations being reported.

Of the remaining 44 patients, 4 had PTCA occlusion of 2 different arteries each for a total of 48 balloon occlusions. In 4 patients the occlusion was of the main diagonal branch of the left anterior descending (LAD) coronary. In 7 patients the occluded lesion was in the LAD distal to the main

diagonal. In 18 patients the LAD balloon occlusion was proximal. Eight PTCA occlusions were in the left circumflex (LCX), 5 were in the obtuse marginal, 1 in the distal LCX and 2 proximal to the obtuse marginal. The PTCA occlusion of the RCA in 11 patients was in the midportion in 8, and the distal RCA in 3. ST 70 data was grouped and tabulated for 5 arterial subdivisions, 1 for each of the 3 LAD distributions, 1 for the LCX, and 1 for the RCA.

The individually verified amplitude of the ST 70 segment in the median beat of the signal averaged ECG was tabulated for each of the 16 leads and plotted on a worksheet showing the location of each lead in the body surface map format of Figure 8. Body surface equipotential map distributions of the ST 70 from the median beat was constructed manually and compared to the 12 LV segment distribution of the model projections of each segment displayed in Figure 8. These distributions were compared to an overlay of each patient's own coronary distribution to each of the 12 segments.

TABLE 1. MODEL SCALE FACTORS (Correction for Proximity Effects)

1: 2.0	2: 2.0	3: 2.0	AVR: 3.5	AVL: 2 0	AVF: 2.0
V3R: 2.0	V2: 1.4	V3: 1.0	V4: 1.0	V5: 1.0	V6: 1.5
LAX: 2.5	LSC: 2.5	V8: 3.0	MB: 3.0		

The ST 70 amplitudes were then scaled to correct for the distance and/or proximity effects from the heart to each lead. For this purpose the scale factors for each lead defined in Table 1 were applied. The scale factors were derived from comparing amplitude of the unit dipole projections from each LV segment to the thorax surface (see Fig. 9) as described in earlier publications (34, 35) and in the 1985 USAFSAM Technical Report (31). The relative amplitudes of the scale factor for each lead was established by taking the peak values of the local anterior segments in the anterior leads V3, V4, and V5 as unity. The upper and lower anterior and the posterior leads were scaled upward to normalize them to the same relative local segment strength as the anterior and apical segments. The scaled ST 70 amplitudes were plotted on the body surface map format. Body surface equipotential maps were constructed manually and compared to the coronary distribution to each left ventricular segment.

RESULTS

Two hundred eighteen PTCA occlusions were performed in 46 patients ranging from 2-10/patient, mean 4.7/patient. Four patients had PTCA of 2 vessels each. Inflation times were typically 1-2 min and varied from 0.25 -5.0, mean 1.6 min. The balloon occlusion showing the greatest departure of the median beat ST 70 in the 16SL ECG from the baseline record prior to each occlusion was taken for analyses. The stability and reproducibility of the recording and median beat methodology was evaluated by examining the variance in the ST 70 amplitudes in each of 2 sets of the 16 leads recorded at the

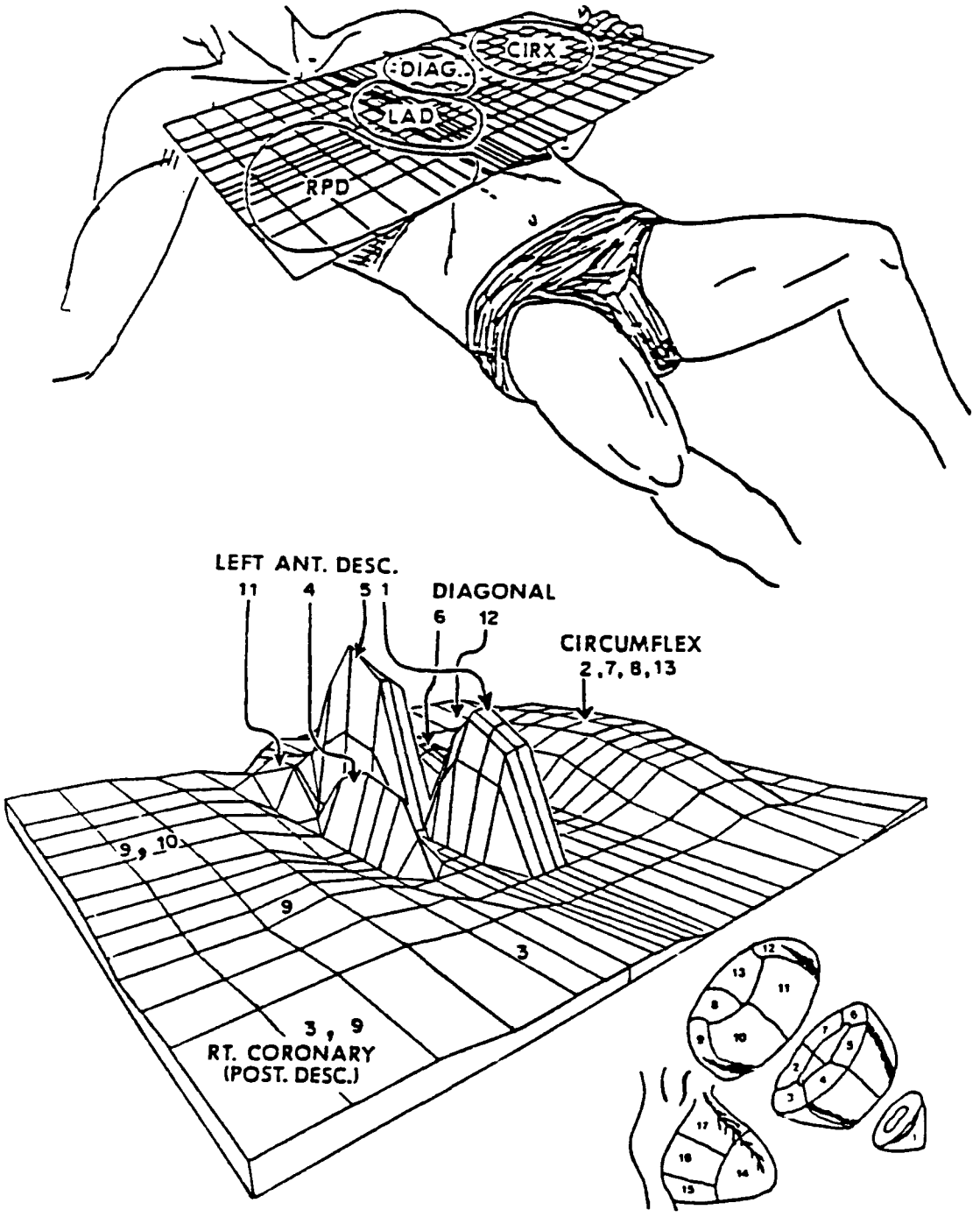

Figure 9. In this illustration the surface distribution of all the left ventricular unit dipoles (clipped at 50% of the positive potential of each segment in the lower right figure) are projected onto the surface. The coronary artery supply to each segment is shown at the top. Note, that in the lower panel the local distribution of each of the segments is well preserved. The height of each segment distribution shown is related to the sensitivity of the ECG surface map to the local left ventricular region.

TABLE 2. PTCA OCCLUSION OF 5 ARTERIAL SEGMENTS (SCALED FOR PROXIMITY EFFECTS) MEANS AND RANGES IN MM (μv/100) OF ST 70 FOR EACH LEAD OF 16SL ECG

LEAD	ART. LAD Diagonal	LAD Distal	LAD Proximal	RCA	LCX
	n = 4	7	18	11	8
1	1.6 (1.0, 2.4)	1.8 (-0.4, 8.4)	2.5 (0.0, 10.6)	-1.3 (-3.4, 0.6)	-0.5 (-2.8, 1.2)
2	-0.1 (-1.4, 1.2)	3.1 (-0.2, 12.2)	0.8 (-2.6, 8.4)	2.1 (-1.4, 9.2)	0.4 (-3.4, 4.8)
3	-1.8 (-2.8, -1.0)	1.5 (-2.2, 11.2)	-1.9 (-12.0, 1.2)	3.5 (0.0, 12.2)	0.9 (-2.8, 5.2)
AVR	-1.1 (-3.2, 0.0)	-4.2 (-11.6, 0.7)	-2.8 (-15.8, 1.8)	-0.5 (-5.3, 2.5)	0.7 (-3.2, 6.0)
AVL	1.6 (1.2, 2.0)	0.2 (-4.8, 5.2)	1.9 (-2.2, 11.2)	-2.4 (-8.0, 1.0)	-0.9 (-3.0, 1.2)
AVF	-0.8 (-2.0, 0.0)	2.2 (-1.0, 11.4)	0.5 (-7.0, 3.4)	3.0 (-0.4, 11.0)	0.3 (-2.8, 4.6)
V3R	-0.8 (-1.6, -0.4)	-0.7 (-3.8, 2.0)	-0.7 (-4.8, 1.0)	0.8 (-0.2, 2.0)	-0.2 (-1.6, 0.8)
V2	0.3 (-0.3, 0.8)	1.4 (0.4, 3.6)	1.5 (-0.7, 4.9)	-1.5 (-5.0, -0.1)	-1.1 (-2.4, -0.1)
V3	0.2 (-0.2, 0.5)	1.9 (0.0, 5.6)	1.7 (-0.1, 4.6)	-1.0 (-4.0, 0.0)	-1.0 (-1.6, -0.2)
V4	0.5 (-0.5, 1.3)	1.9 (0.2, 6.4)	1.5 (-1.2, 5.1)	-0.6 (-2.0, 0.0)	-0.6 (-1.9, -0.1)
V5	0.4 (-0.6, 1.0)	0.3 (-0.4, 1.4)	0.4 (-1.4, 2.0)	-0.1 (-0.5, 0.3)	0.3 (-0.6, 1.6)
V6	-0.2 (-0.9, 0.2)	-1.4 (-3.2, 0.0)	-0.7 (-4.8, 0.8)	0.5 (-0.9, 3.9)	1.5 (0.0, 3.0)
LAX	1.8 (0.5, 4.3)	-1.6 (-5.5, -0.3)	0.1 (-5.0, 5.0)	-1.1 (-4.8, 0.5)	1.5 (0.5, 3.3)
LSC	-1.8 (-2.0, -1.5)	0.6 (-3.3, 3.0)	-0.4 (-6.5, 4.0)	2.5 (-0.5, 8.8)	-0.3 (-3.5, 2.0)
V8	-0.6 (-1.5, 0.3)	-3.7 (-9.6, -0.3)	-2.8 (-11.4, 0.3)	1.6 (-0.9, 12.6)	2.8 (0.9, 6.3)
MB5	-0.6 (-1.2, 0.0)	-4.4 (-11.1, 0.0)	-3.0 (-12.0, 0.6)	2.6 (0.0, 14.7)	2.5 (0.6, 5.4)

beginning of each study. Established from these data (16 x 46 pairs) the 98% confidence limit of reproducibility of the measurement on the baseline tracings was ± 20 μv. The 2 excluded asymptomatic subjects fell within these bounds. The PTCA balloon occlusions of individual coronary arteries each resulted in maximal elevation of the ST 70 segment in leads predicted by the forward model to be specific for the arterial perfusion bed of the vessel occluded. The manually constructed body surface equipotential maps from the median beat ST 70 data were then reviewed. We noted in leads more distant from the heart, even though there was significant ST change, the potential maxima

were often displaced from the area projected for the local regions by the unit dipole transfer impedances. The amplitudes of the recorded ST 70 in all leads were then scaled to the relative amplitude of the unit transfer impedances shown in Table 1. These data are summarized in Table 2. Maps constructed from these data confirm the forward model predictions. They were consistent with the hypothesis that, when corrected this way for local proximity effects, body surface ST 70 change localizes to the region of the map specific for the local segment. The sum of the ST 70 in each lead showing ST elevation of greater than the 20 μv reproducibility standard was accumulated for each of the 5 coronary arterial subsets described. The means of the ST 70 change in each lead was computed and displayed as a 3D plot on the perspective display of the surface map as shown in Figures 10 and 11. These plots was done to compare the relative ability of the local surface leads scaled as just described to predict the local current of injury from each of the 5 regions.

From a review of Table 2 we noted that, when scaled to correct for proximity effects, the peak amplitude of ST elevation (injury current) was seen in 1 of the 4 extra leads in 16 (33%) of 48 PTCAs in 44 patients. From a review of this data, and the perspective plots of Figures 10 and 11, the following observations can be made: In the 4 patients with occlusion of the main diagonal branch of the LAD, the maximal elevation of the mean ST occurred in the left axilla and left upper chest with major ST depression in inferior leads, and minor ST depression or no significant change in back leads and V6; occlusion of the LAD distal to the first diagonal in 7 patients produced local ST elevation limited to the anterior precordium, with the same maximal average amplitude in V2, V3, and V4, minimal ST elevation in V5 none in V6 and significant depression in the axilla, and on the back; PTCA occlusion of the LAD proximal to the 1st diagonal in 18 cases produced a combination of these effects with average ST elevation maximal in the left upper torso, little or no change in V6, and ST depression in back leads; in the 8 patients with left circumflex occlusion the maximal of the averaged ST elevations localized to the back in 7, and to the left axilla in 1, with significant ST elevation in V6 and ST depression in anterior leads; RCA occlusion in 11 produced the maximal elevation of the average ST currents of injury in the inferior leads. There was ST elevation in the posterior leads (in all but 3) that was proportional to the posterior extent of the distal posterolateral branch distribution in each case. The expected mirror image ST depression in anterior leads V2 and V3 and the upper left anterior torso was also observed.

The 1 patient described earlier (but not included in the 44 just described) who developed persistent angina in the laboratory at the time of guide wire insertion through a proximal LAD stenosis had persistent ST depression associated with the angina throughout. The earliest onset of mild chest pain was associated with ST depression in AVF of a very small amplitude of 20 μv net change. As the pain became more severe the ST change became most pronounced in anterior leads V3-V5 with the maximal change of 220 μv in V4 and classic downsloping ST segment depression. The distribution of these ECG changes was the same as the 18 patients with total balloon occlusion in the same arterial segment as this patient's hi-grade LAD lesion. The patients with PTCA occlusion all had ST elevation in these leads and this patient had ST depression. Intracoronary injection of contrast showed distal filling of the LAD around the guidewire. At no time did the artery appear to be totally

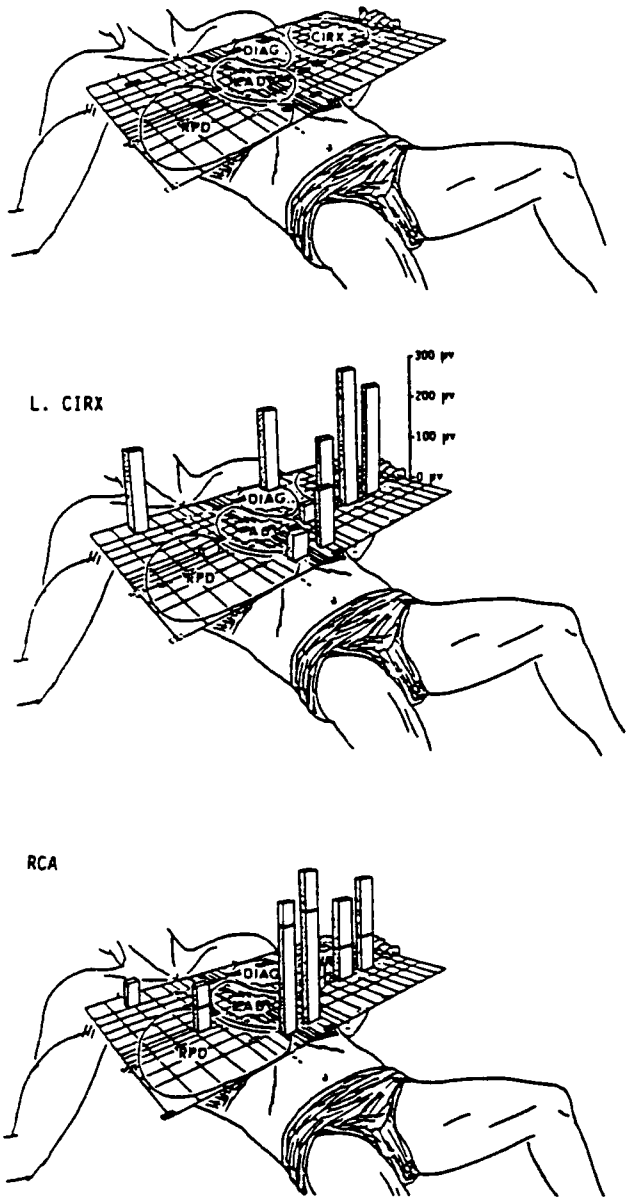

Figure 10. Body surface projection seen in perspective, and distribution of ST 70 ms after J point (positive potentials only) in each lead of the 16SL system. The black rectangles in the top panel show the lead locations used in this study. The distribution of the regional arterial perfusion beds, as predicted by the simulation, is reproduced from Figure 9 for reference. The distribution of the positive mean ST 70 (relative height of the vertical bars in the middle and lower panels) is shown during left circumflex (L. CIRX) occlusion in 8 patients, and RCA occlusion in 11 patients. Significant localization of the mean ST 70 elevation is seen as follows: LCX in leads LAX, V8, MB5, and V6 (with the maximum in V8); RCA in leads V3R, LSC, AVF, V8, and MB5 (with the maximum in AVF).

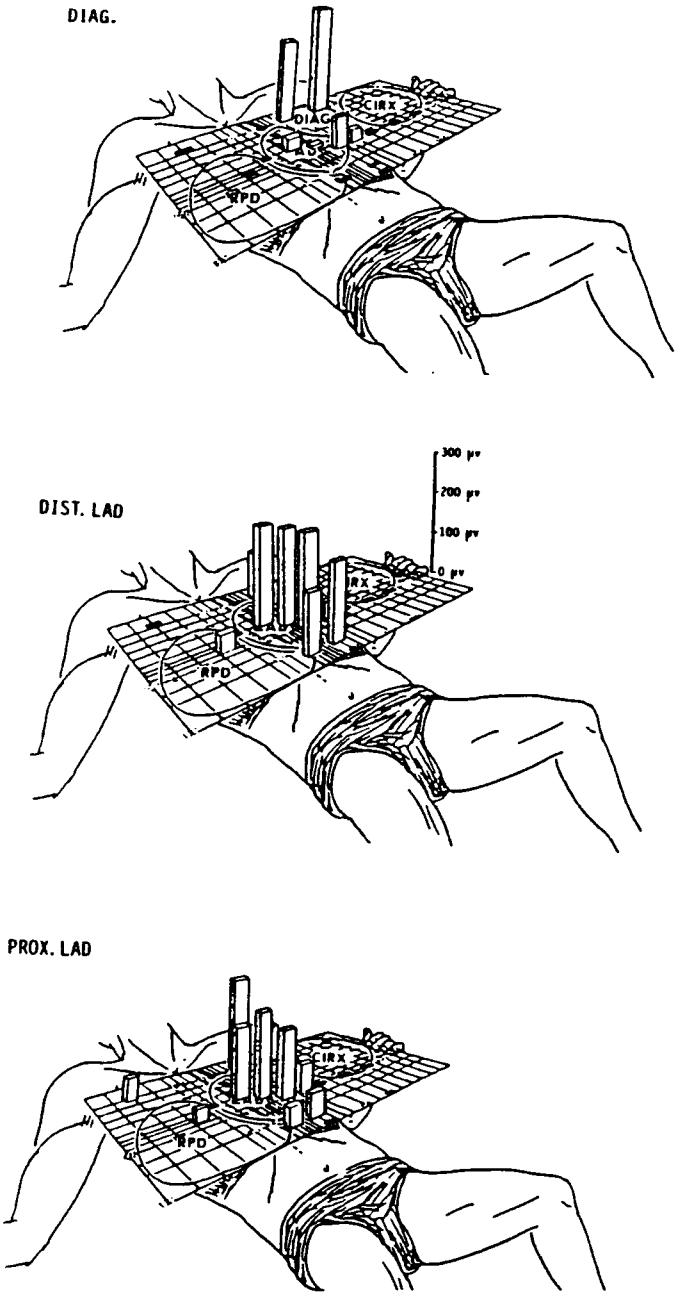

Figure 11. The mean ST 70 elevation (positive potentials only) in each lead is shown by the relative height of the vertical bars during PTCA balloon occlusion of the LAD system. Note also, the mean ST 70 distribution in the 3 panels with occlusion of Diagonal (DIAG) in 4 patients, Distal (DIST) LAD in 7 patients, Proximal (PROX) LAD in 18 patients, respectively. Significant localization of the ST 70 elevation is seen as follows: DIAG LAD in leads AVL and LAX; DIST LAD in leads V2-V4, AVF; PROX LAD in the combination of the above leads.

occluded. The pain and ST change responded incompletely to intravenous nitroglycerine drip, the ischemic STT changes persisted, and after several unsuccessful attempts to pass various balloon catheters past the obstruction the patient was referred to the surgeons for urgent bypass surgery which was accomplished without incident.

DISCUSSION

These data verify predictions from the Forward Model Simulations and support the hypothesis that significant additional resolution and sensitivity to ischemic change is to be expected with a broader lead array. The extra lead in the axilla was strongly positive for ST injury with diagonal and circumflex occlusion in the present PTCA study. It separated this group from those with both distal LAD and RCA occlusion. The proposed 30SL lead array adds an extra lead on the left upper back 10 cm above the V8 position. We expect this lead to discriminate between the LCX and the diagonal distributions and along with V8 to be the most sensitive to ischemic changes in the obtuse marginal distribution. The mid-back lead was most sensitive to basal ischemia in both the RCA and LCX balloon occlusions but did not distinguish them well from each other. The new back leads at the V8R position and high on the right back above it are expected to be most sensitive to ischemia (and/or infarct) in the high posterobasal regions of the left ventricle. These two leads also complete the back leads for the Grishman Cube System, which in the Rancho Database (36,37) was most sensitive to infarct and ischemia in this distribution.

Interestingly, in the PTCA studies lead V6 ST changes consistently tracked with arterial distribution and ischemia to the posterior wall. In the study of 48 PTCAs in the population of 44 patients with demonstrable ischemic change with balloon occlusion, V6 recorded significant ST elevation in 18/19 (95%) LCX and RCA occlusions. In the 11 distal LAD or diagonal occlusions none had ST elevation, but 7 had significant ST depression (from 30-300 μv) in V6 as well as in both back leads. In the 18 proximal LAD occlusions, V6 showed no demonstrable ST change in 4 cases in spite of major ST elevation in the anterior V leads; 12 had ST depression in V6 ranging from 30-480 μv and even more ST depression on the back; and 3 had ST elevation of 30-80 μv. Thus, only 3/29 (10%) of the total patient group with LAD occlusion had demonstrable ST elevation ranging from 30-80 μv whereas 7 (24%) had no demonstrable change and 19 (66%) had ST depression ranging from 30-480 μv. We also observed in the modeling studies of subendocardial ischemia (and/or infarction) that V6 change (ST depression) was seen with ischemia in the obtuse marginal circumflex distribution, whereas with subendocardial ischemia in the distal LAD distribution there was little if any change, or slight mirror image ST elevation seen in V6. ST depression began to appear in V6 only when there was major apical posterolateral ischemia extending well up towards or into the midregion.

The angioplasty studies demonstrated ST elevation in V3R with occlusion of the RCA (9/11 PTCAs) and it was most marked when the occlusion was proximal to the acute marginal branch supplying the right ventricle. There was similar ST change (7/29 patients) with LAD occlusion associated with major change in V2-V4. These changes may represent ischemia of the base of the septum. From

these observations, the Kornreich studies, and the simulation studies we expect the added leads on the right thorax will improve the sensitivity to ischemic change in the base of the septum and in the right ventricle. The V4R lead in the new 30SL system completes the Grishman Cube lead system and based on the Rancho database referred to earlier (36,37) should increase the sensitivity to both posterolateral wall change and the balance between it and the right ventricle.

There were 2 major limitations to this local coronary artery balloon occlusion study using the 16SL ECG system. First, the electrode array was limited to 4 additional ones to the conventional 12-lead ECG. Since the 12SL ECG is made up of 8 independent leads from which 4 limb leads are computed, the 16SL ECG used in our study is made up of 14 electrodes and 12 independent leads. The prior studies with the forward model had suggested that a 22 electrode array of 20 independent leads might be the optimal electrode array for detecting "silent" ischemia in the asymptomatic pilot population. The present study suggests the need for electrodes in added locations not suggested by the earlier model studies. The multigroup discriminant function studies of Kornreich et al., have also suggested the need for electrodes in additional locations. The location of these extra electrodes (shown in Fig. 5) currently being recorded with the 30SL ECG is a synthesis of these 3 lines of study. The second major limitation of our study is that, except for the subjective chest pain and the ST change on the 16SL ECG, there is no independent objective measure of the degree of ischemia in the distal arterial perfusion bed produced by each of the coronary occlusions. The distribution of the coronary artery tree distal to the occlusions can be defined, but how much of this perfusion bed is ischemic, and the degree of that ischemia, in not known. With the more extensive electrode array of the 30SL ECG system, the forward model will be used to emulate the ECG changes of mild, moderate, and severe ischemic "injury" produced by several typical local PTCA occlusions, and by exercise induced ischemia in these same subjects. From these simulations we expect to refine our earlier recommendations for the optimal number and location of electrodes, as well as the testable hypotheses for optimal criteria in these leads, to detect "silent ischemia."

The increased spatial resolution from the added leads of the 30SL ECG system is expected to improve the detection of these ischemic changes when they occur. The 1-ms sampling rate, and signal processing to reduce noise, defines waveforms in significantly more detail. The higher resolution of each of these 30 individual waveforms that results from this processing, and the ability to display them as 3D body surface isopotential maps, discriminant function maps, spatial or temporal integral maps, etc., over time or in Hi-Fi 12SL (or 30SL) ECGs, and VCGs will further improve the ability to detect these ischemic changes. The sensitivity, specificity, and predictive accuracy of the various parameters derived from this technique, especially as relates to the USAF population will, also be defined. We expect the current 30SL ECG contains redundant electrode locations as far as the detection of "silent" ischemia is concerned. By the use of multivariant techniques on the sampled data, and judicious use of the forward simulation to define the anatomic and physical basis for the observed changes it should be possible to define the minimal set of electrodes for application in the field that will optimize the detection of previously unrecognized coronary disease in asymptomatic aircrewmen.

CONCLUSIONS

Percutaneous coronary angioplasty (PTCA) occlusion in 5 individual coronary artery distributions produced significant ST elevation ("current of injury") in 48/50 such occlusions in 46 patients, 4 of whom had balloon occlusion of 2 separate coronary arteries. Two patients had no significant ischemic ST change in any of the 16 leads recorded and no chest pain in spite of balloon occlusion of a proximal right coronary obstruction and were considered to have no evidence of ischemia. Therefore, in 48 PTCA occlusions in 44 patients all had ST elevation in the leads defined in simulation studies as specific for the arterial perfusion bed involved. The only patient with local ST depression in the regionally specific leads was the patient (not tabulated) with subtotal LAD occlusion and persistent angina in whom PTCA occlusion could not be accomplished. In this case the ST change also localized in the leads specific to the LAD distribution as defined by the simulation studies. These data confirm the prediction of the Forward Model Simulations and add strong support to the hypothesis that additional resolution and sensitivity to ischemic change is to be expected with a broader array of ECG leads. Continued work with the 30SL ECG system now going online, along with judicious application of the forward simulation, should define the optimal number of leads, electrode location, and optimal criteria in these data for the detection of unsuspected ischemia in asymptomatic aircrewmen.

RECOMMENDATIONS FOR THE ONGOING EFFORT

The Hi-Fi 30 simultaneous lead electrocardiographic (30SL ECG) digital data acquisition system, described in detail in Task 3 to follow, now performs as designed to meet the scientific objective of this task. The system includes the remaining 4 limb leads that are computed from the 2 that are recorded and thus has 26 independent leads. This system digitizes at a 1-ms sampling rate, cycle selects for the typical beat, and signal averages to reduce noise. From these 30SL Hi-Fi ECGs detailed analysis of all ECG components will now be possible. This analysis includes individual high amplitude waveforms, Hi-Fi 12SL ECGs, 30SL ECGs, Frank, McFee, or Cube Vectorcardiograms, body surface potential maps, temporal and/or spatial frequency transform maps, Kornreich's discriminant function maps, etc. We have documented in earlier studies of coronary artery disease patients (10) that serial Hi-Fi, simultaneous, signal processed ECGs and VCGs detect new infarcts (1/3 of which are silent) with a 98% confidence. The present Hi-Fi 30SL ECG system is a specific outgrowth of this experience and is directly applicable to the task of detecting unsuspected coronary disease, i.e., new "silent infarcts" in the asymptomatic pilot population with a similar (98%) level of confidence.

The task for the immediate future year is to define the optimal lead number, location, and criteria for the detection of "silent ischemia." Various ECG parameters proposed in the past as related to ischemia will be systematically examined with the 30SL ECG system and its various subsets and transforms. These parameters include: 1) the definition of the relationship of P-wave changes recently demonstrated as being related to ischemic ventricular dysfunction, especially diastolic dysfunction, 2) transient QRS changes postulated to be changes in activation sequence(i.e.,disorders in intraventricular conduction) have been repeatedly observed with transient ischemia from PTCA occlusion, and from exercise stress testing, and 3) the definition of the optimal STT parameters as markers for ischemia will be examined, including ECG J point, ST 40, ST 60, ST 70, ST 80, Mid-ST, Mid-T, time plots of individual lead ST integrals, Max ST integrals, Spatial ST integrals, and total test ST integrals for individual leads or for all 30 leads. We will continue the analysis using the forward simulation to explore for optimal lead number, location, and optimal criteria in these leads and to generate testable hypotheses or criteria for detection of ischemia in asymptomatic subjects. One such set of testable criteria from the earlier forward model studies is discussed in more detail in the Appendix.

To accomplish this task, we will be acquiring Hi-Fi 30SL ECG data over the next few months during exercise testing and angioplasty at the Long Beach Memorial Heart Institute. Our objective is to have both tests available at closely spaced time intervals on most subjects. We will also be accumulating exercise test 30SL data on subjects being considered for coronary angiography. Some of these subsets will have normal coronary arteries. A database from volunteer normals will be accumulated with this new 30SL recording system over the next several months. Early in the coming year when the systems have been field tested at the Long Beach Memorial Heart Institute and operating smoothly we will train an exercise laboratory aircorpman in its use. We will also supervise its installation at the USAFSAM* Brooks AFB, Texas. This supervised

*Redesignated Armstrong Laboratory.

installation will allow for the direct testing of the model hypotheses in the pilot population. Those pilots who have been screened as at increased risk for possible coronary artery disease, but who have angiographically normal coronary arteries, can be considered representative of that portion of this population most likely to have false positive 30SL ECG changes. This group, along with those asymptomatic USAF subjects with documented coronary disease, will be the target population for adjusting the criteria for optimal performance to meet the objective of detecting asymptomatic coronary disease at rest, and with exercise in aircrew persons. During this same time we will continue to accumulate Hi-Fi 30SL ECG data at the Memorial Heart Institute during exercise testing and PTCA. From these two databases we would expect to have enough data by 30 May 1992 to be able to explicitly specify the resolution, sensitivity, and specificity of the 30SL ECG in the aircrew population. With this information it will be possible to accurately define the cost-effective trade-offs for the implementation of such a screening system in the USAF medical system worldwide.

While the current version of the 30SL ECG recording system is appropriate and adequate to obtain the data necessary for the scientific purposes of this contract it is not, in its present form, an optimal system for routine screening and testing to be installed in the field. By the end of the current year's contract we will have been able to correct some of these limitations and will be able to specify in detail the specifications of an appropriate routine ECG/Exercise test screening system.

SUMMARY AND CONCLUSIONS

Based on the analyses presented in the Overviews and Objectives, (both the Clinical and U.S. Air Force Perspectives) at the beginning of this report, the identification of even 1 in 10 pilots of high-performance aircraft with totally unsuspected coronary disease will save the government $3-$5 million per year by preventing loss of aircraft and pilot from sudden death at the controls of an aircraft. In his overview, Tolan reports that there are about 50 acute myocardial infarcts per year documented in rated flying presonnel. There can be little doubt that an equal number of acute myocardial infarcts go unrecognized and unsuspected. Half of these "silent infarcts" would be recognized by conventional criteria on routine followup standard 12-lead ECGs, but by the data developed in the Framingham autopsy study, the other half would be classified as completely "silent." From earlier analysis of the data in hand (10), and the data presented herein, serially recorded Hi-Fi 30SL ECGs are now capable of identifying most, if not all, of these new "silent infarcts" which are not detected with routine serial 12-lead ECGs. The improved detection of "silent ischemia" will follow with continued enhancement of the system as outlined herein. We expect the routine worldwide screening of the pilot population with this Hi-Fi 30SL ECG system, at rest and with exercise testing, to detect significantly more than 1 in 10 (conservatively at least 5 in 10) pilots each year with significant coronary disease that are not now being identified. This recognition would result in major salvage of key personnel and an estimated savings overall of $15-$25 million annually.

TASK 3: 30SL HI-FIDELITY ECG DATA AQUISITION SYSTEM AND LEAD LOCATOR SYSTEM

Design of the 30SL ECG Digital Data Acquisition System

System Components. (Block Diagram, see Fig. 12)

(1) Everex Step 286/20 Personal Computer (PC).
(2) Mortara Instrument PCECG boards.
(3) Z-200 fanfold writer.
(4) Hard disk and floppy disk drives.
(5) QIC tape cartridge drive.
(6) Color monitor.

Specifications.

(1) The STEP 286/20 contains a 20 MHz 80286 16-bit microprocessor. Memory management architecture is a write-back cache which delivers effective zero wait-state operation with 2 MB of main memory on the system board. An IIT-2C87 math coprocessor running at 20 MHz is installed on the system board. Hardware speed switch provides 3 central processing unit frequency settings: 20 MHz, 10 MHz, and 6.7 MHz. The system board has six 16-bit and two 8-bit automatic transmission (AT)-compatible input/output (I/O) bus slots. An EEPROM permits selectable I/O bus speeds of 8 MHz and 10 MHz. Power comes from a 200-w power supply, switchable between 110 and 220 v.

(2) PCECG boards are 8-lead, isolated input, PC/AT-compatible circuit cards. Patient input leakage current is less than 10 μa per input card. Analog data acquisition is at 1,000 samples per second for each lead, 1.25 μv least significant bit, +/- 20 mv dynamic range, +/- 300 mv direct current (DC) offset tolerance, 31.25 μs interchannel skew with a maximum of +/- 125 μs. Filters consist of a single-pole 4.096 second (0.04 Hz) high pass to control baseline and a 50/60 Hz alternating current (AC) interference rejection filter.

(3) The Z-200 fanfold writer operates in the raster frame graphics printer mode with a total of 1,728 thermal elements. Text mode uses a 24 vertical position font size. Each raster frame is sent from the parallel port at 500 Hz.

(4) A Data Technology Corp DTC-6280 high performance 1:1 interleave ESDI hard/floppy disk controller is installed in combination with a 1.2 MB floppy disk drive (FDD) and a Maxtor 4170E ESDI 179 MB capacity hard disk drive (HDD). The HDD transfer rate is 10.0 M bits/s, typical seek time is 14 ms average, 2.5 ms track-to-track, and 27 ms full stroke. Formatted capacity at 512 bytes/sector is 157.93 MB.

(5) The Everex streaming tape drive and controller are AT compatible QIC format. The system uses the equivalent of 3M DC600A cartridge with a capacity of 60 MB. Backup is at 5 MB/min without the need for pre-formatting. Menu driven utility software provides easy-to-use backup, restore, and compare functions. Both image and by-file methods are available.

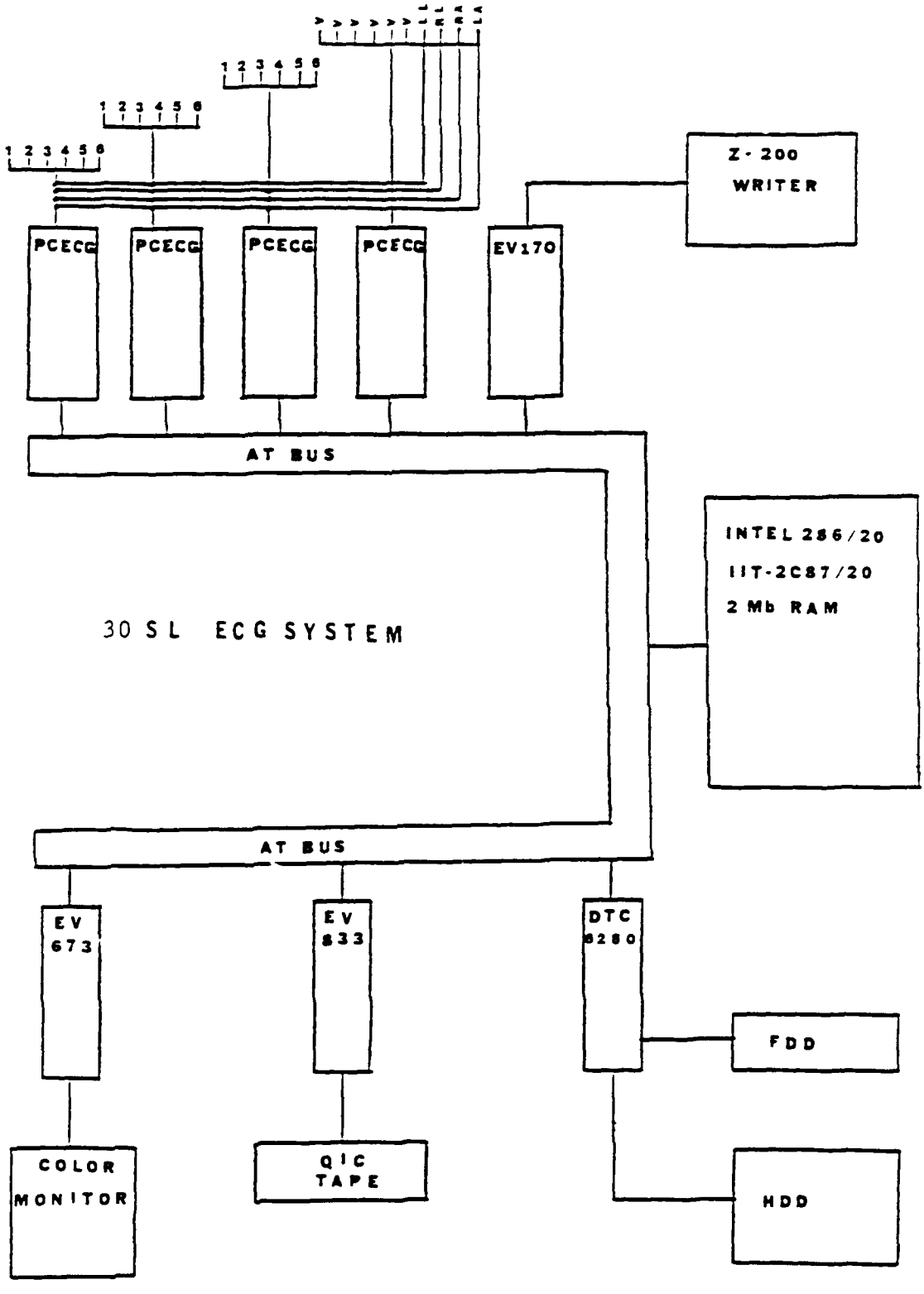

Figure 12. ECG data acquisition system with 30 simultaneous leads. A set of 4 PCECG cards and 4 device controllers are connected to an AT bus of an Everex 286/20 PC.

(6) A color monitor and VGA adapter provides a resolution of 800 dots horizontal, and 560 lines vertical. Horizontal synchronization is 15.6 kHz to 36 kHz automatically, vertical synchronization is 45 Hz to 90 Hz automatically. Display area is 245 mm horizontal and 184 mm vertical. Video bandwidth is 30 MHz. Cathode ray tube (CRT) has 0.31 mm trio dot pitch with P22 medium-short persistence.

Software.

(a) Coprocessor (68.000) hex file.
(b) Download program (pcload.c).
(c) Common declarations and definitions (usafcom.h).
(d) CRT format definitions (crtdef.h).
(e) Writer format definitions (wrtdef.h).
(f) Main program (usaf.c).
(g) Keyboard monitor (kbmon.c).
(h) CRT display generator (setcrt.c).
(i) CRT pixel generator (crt.c).
(j) Writer format generator (xrprint.c).
(k) Writer raster generator (raster.asm).
(l) Input FIFO controller (fifo_irq.asm).
(m) Graphics image data transfer (xfrcol.asm).
(n) Writer/printer interface control (cipio.asm).
(o) Large-character font for CRT and writer (crtfont.asm).
(p) Miscellaneous library (misc.c).
(q) Color palette control (loadpal.c).
(r) "make" files (mkusaf and usaffil).

Operational Characteristics.

Signal processing characteristics include QRS detection, dominant rhythm cycle identification at each 10 s interval, dominant cycle averaging over 10 s, 900 sample average cycle (1 s with QRS centered at 400 ms point), and QRS onset/offset detection for each average. Display processing consists of an 8-lead rhythm display and an 8-lead average cycle display. On screen display shows 4 leads for 2 s on the left half of the monitor, followed by the other 4 leads for 2 s on the right half of the screen. On the far right of the monitor screen, 2 columns of 4 each display the 8 leads of 10 s averaged data. Function keys [F1], [F2], [F3], and [F4] switch between the 4 PCECG boards. Leads I and II are repeated for each display as the boards are switched. Pressing function key [F5] produces a hard copy of the next 10 s of all 8 leads selected for display on the monitor, including the averaged cycle. Lead labeling, patient name, date/time, and board number are printed on the form. Examples of a typical hard copy for each of 4 banks of 8 leads are shown in Figures 13-16.

On-line storage of 3 rhythm leads (I,II,V5), and the 26 lead averages for each 10 s interval is to the HDD. Leads I, and II are repeated with each bank of 6 chest leads. The 4 remaining limb leads are computed off-line from the 2 recorded. The capacity of the HDD permits continuous recording for 166 min. From a rapid screen post-processing survey of the stored data, requested sets of 30SL ECG median data is plotted by laser printer. Data archiving is done off-line to a 60 MB streaming tape drive using the Everex utility software.

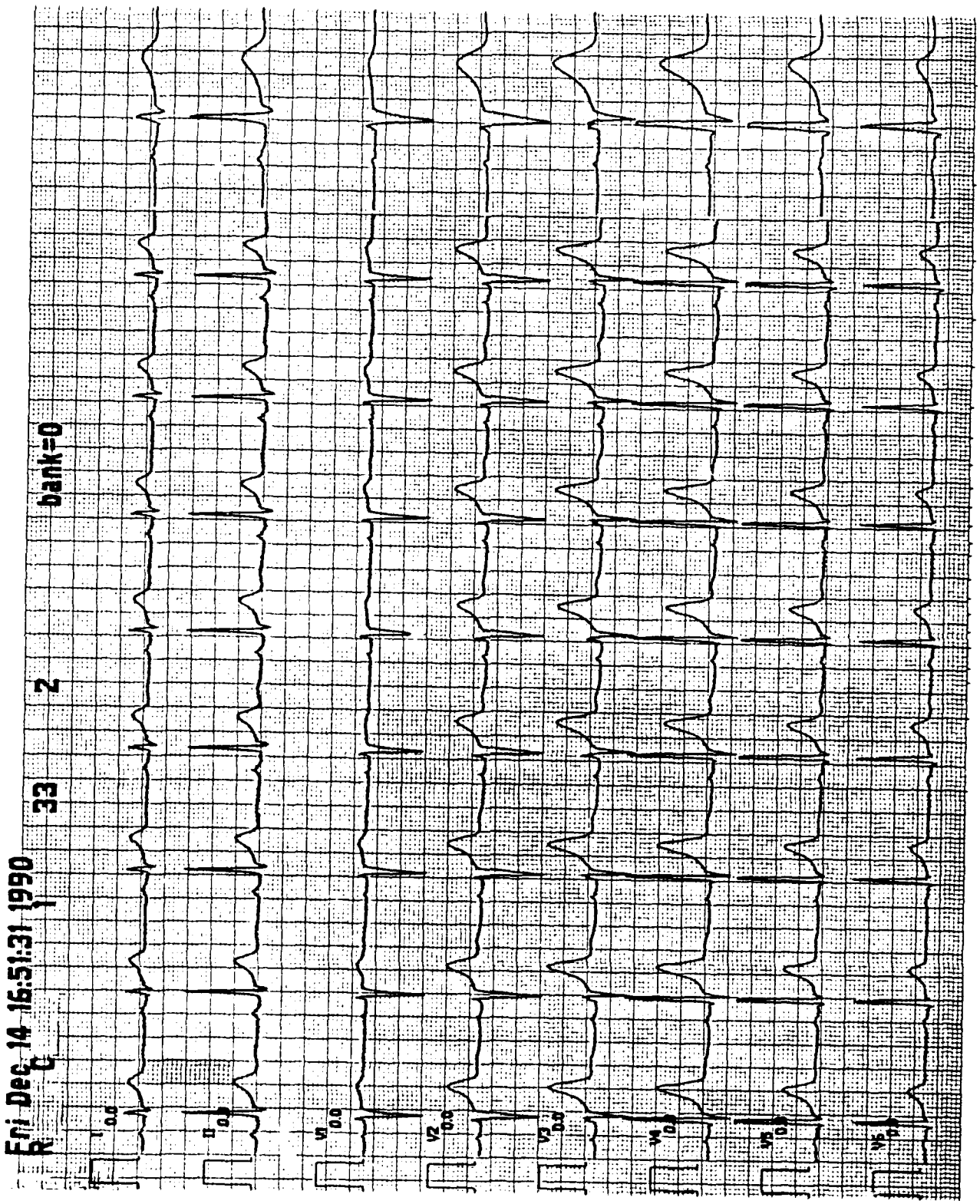

Figure 13. Bank 0: Electrodes are applied to standard limb leads I and II in this bank and in banks 1-3 to follow. V leads are applied to the standard precordial leads V1-V6.

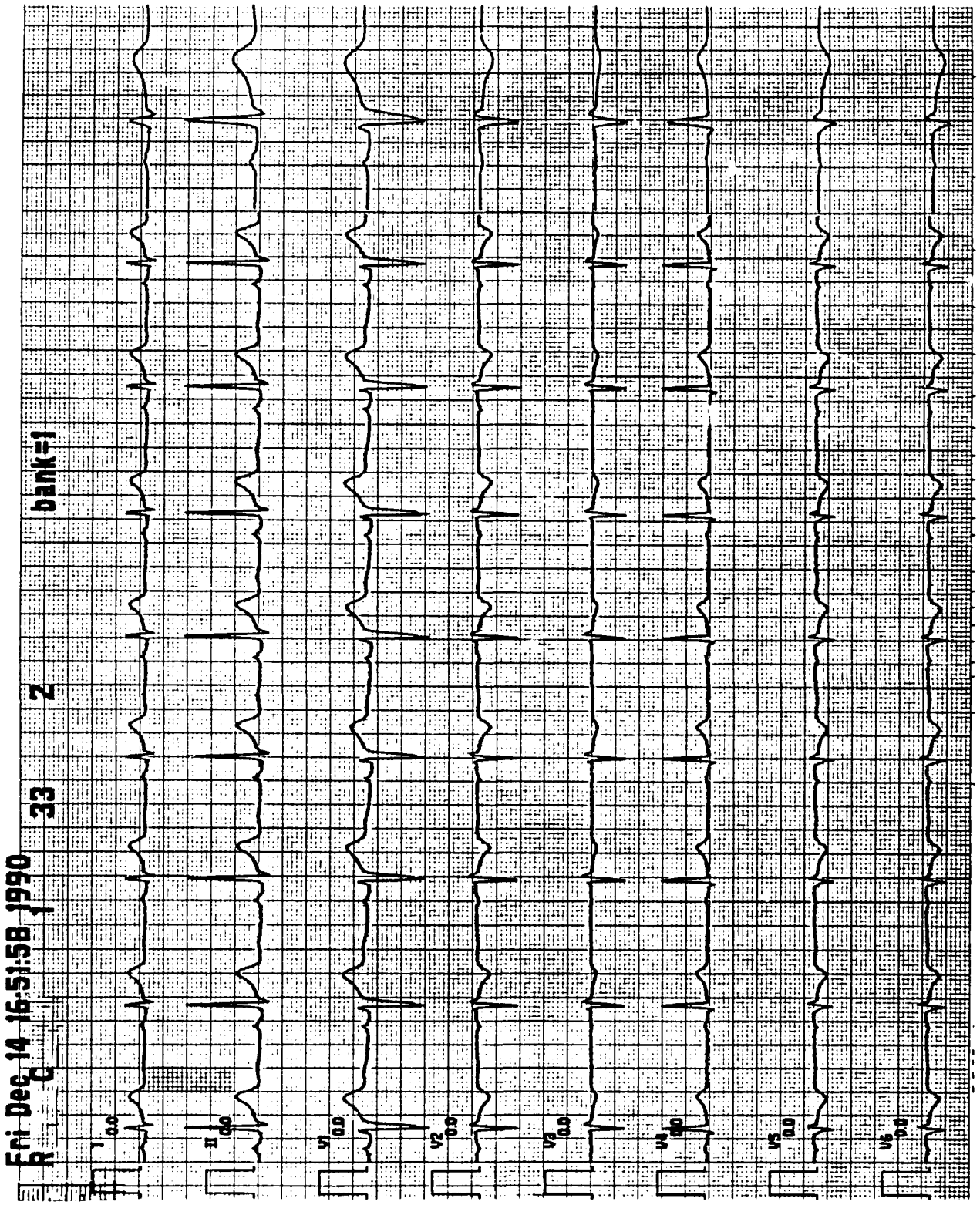

Figure 14. Bank 1: Electrode V1 is applied at the midsternum at the horizontal level of standard V4. V2, V3, and V4 are applied 10 cm above standard V1, V2, and V4, respectively. V5 is applied on the back of the neck at cervical 7, and V6 on the back right mid-clavicular line 20 cm above the level of standard V4. (see Fig. 5)

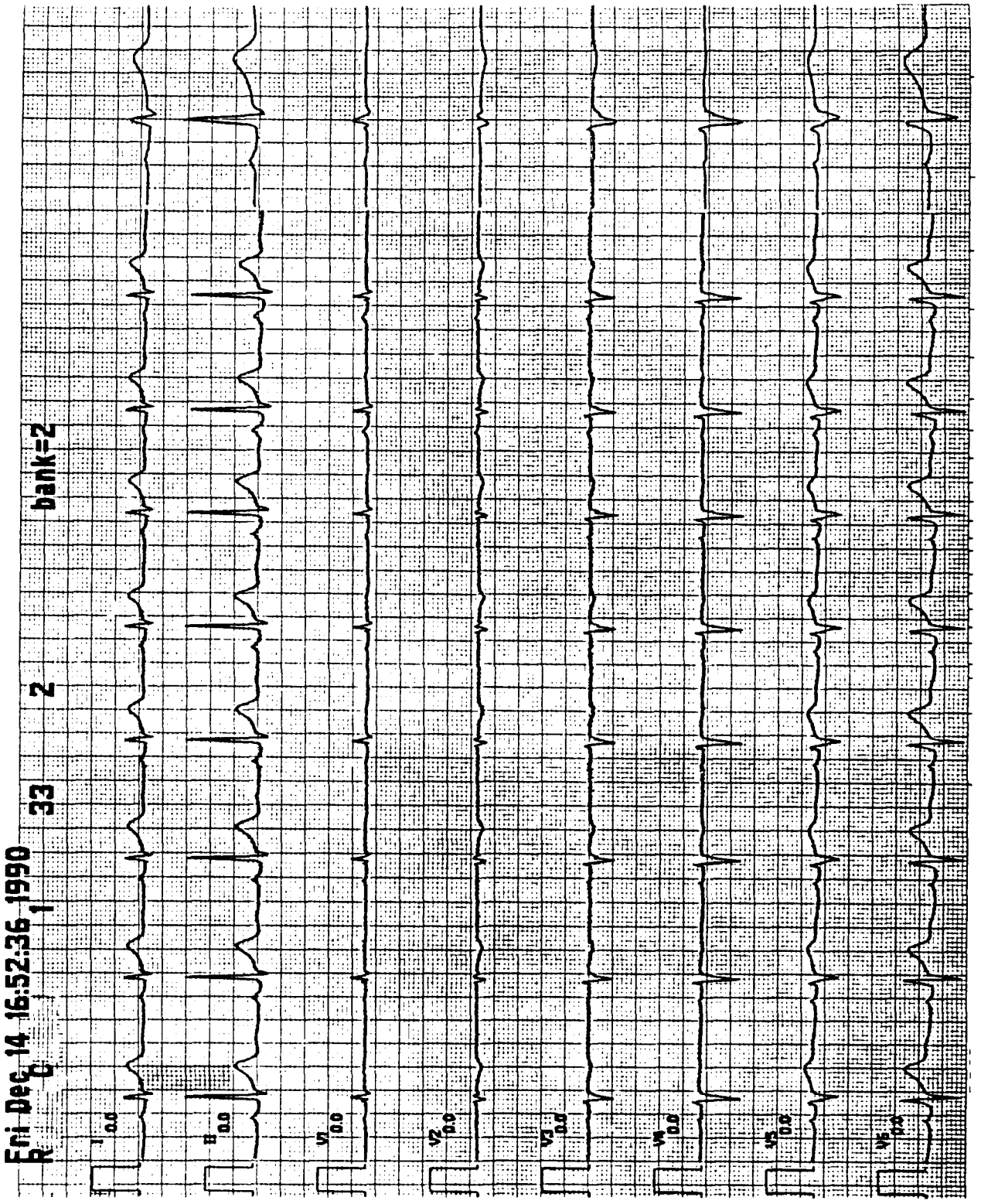

Figure 15. Bank 2: Electrode V1 is applied 10 cm below V6R, V2 is located at V6R in the right anterior axillary line (at the level of standard lead V4). V3 is located at the V4R position, V4 at V3R, V5 and V6 10 cm below standard V1 and V2, respectively (see Fig. 5).

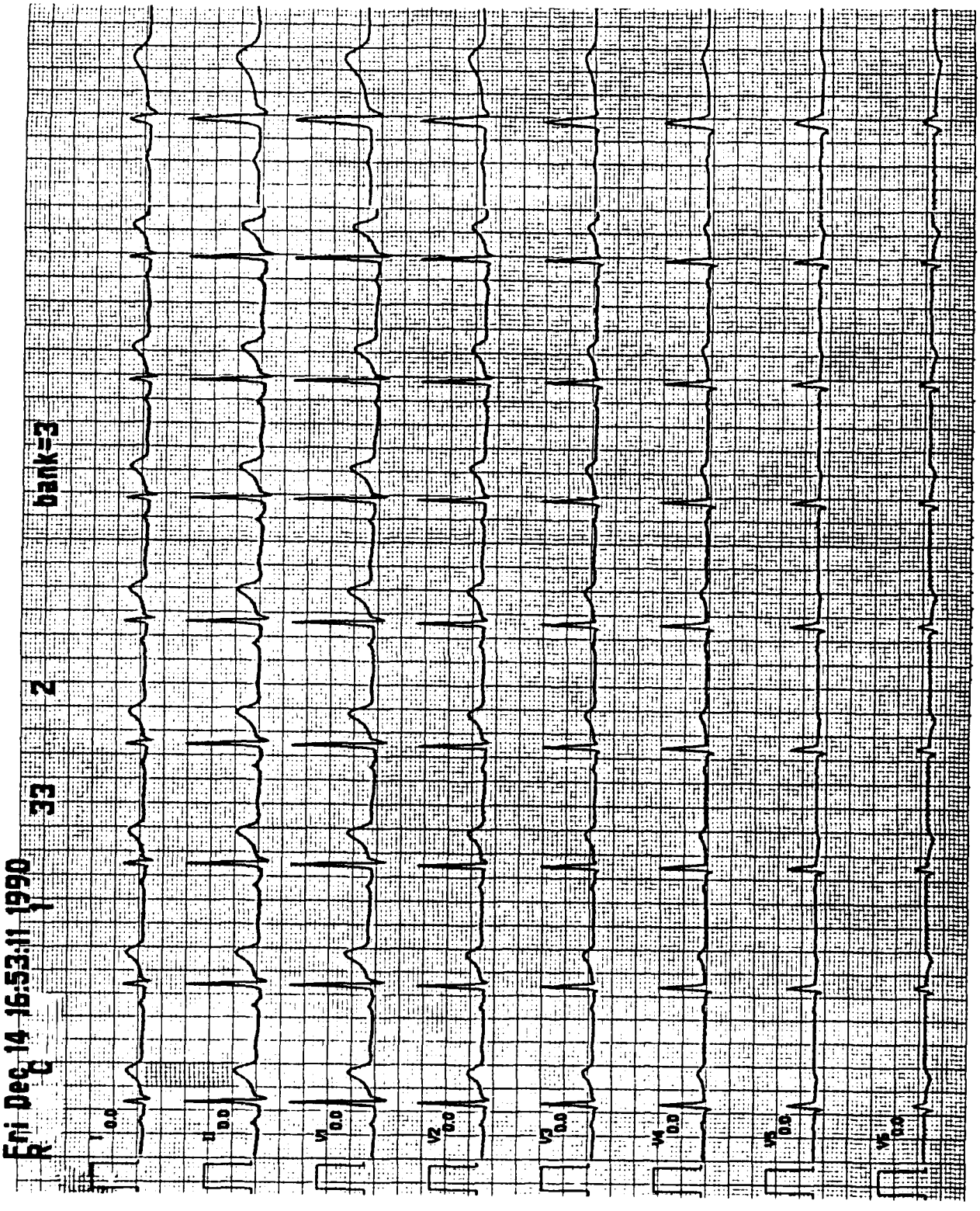

Figure 16. Bank 3: Electrodes V1, V2, and V3 are applied 10 cm below standard V4, V6, and V8, respectively (V8 is on the back directly posterior to the standard V4). V4 is applied at V8, V5 is on the midback, and V6 at V8R, both at the level of standard V4 (see Fig. 5).

Prototype Electrode Locator

System Design and Schematic.

The prototype electrode locator (see Fig. 17 for schematic) was designed to meet the following criteria:

(1) Output a constant amplitude current of 10 μa to a pair of chest electrodes.
(2) A sinusoidal frequency of 100 Hz with maximum distortion of 0.2%.
(3) Output pulse duration of 1 s.
(4) Electrode lead choice switch selectable over 4 sets.
(5) Electrode-to-skin impedance of the lead is required to be less than 15 kohms.
(6) Battery operated with a source voltage of 15 VDC.
(7) Portable with short patient cables (2 ft, 0.61 m).

Subject Test.

A prototype lead locator was tested in a 33-year-old male subject in normal health. The 3 leads selected were: 1) anterior-posterior at the level of the xiphoid process, 2) right-left axillae at the same level and 3) vertical axis from the left midclavicle and a point in the left midclavicular line at the level of the xiphoid. Electrode characteristics of each of the 3 leads were measured after site preparation and found to have the following properties:

(1) Anterior-posterior lead had an offset voltage 16.9 mv and an impedance of 2.3 kohms.
(2) Right-left lead had -1.1 mv offset and 0.5 kohms impedance.
(3) Vertical lead had -2.5 mv offset and 13.5 kohms impedance.

Figures 18, 19, and 20 are of these same 3 leads in the order of A-P, R-L, and Vertical. ECG leads I, II, and V1-V6 with a 10 s average from the same PCECG board are displayed for all 3 current injection episodes. The 100 Hz oscillator current lasts for 1 s in each case and the amplitude varies across the conventional ECG leads differently for each of the current injection leads. These variations establish the relationship of the chest electrodes to one another and will be used to test for incorrectly placed leads of the 30SL system before collecting data. The orthogonality (separation of effect) between many of the leads is apparent in these 3 tracings.

Selecting an optimum set of electrode locations on the chest to inject the current and produce maximum orthogonality in the 30 leads must be moderated by the need to select a set of locations with clearly identifiable landmarks. Repeatable locations for the current stimulation leads are a necessity because the procedures for locating misplaced ECG leads assumes the correct location of the stimulating sites. Computer program procedures for locating misplaced ECG leads does not depend on specific stimulation sites; however, the ability to locate misplaced leads will depend on the signal separation

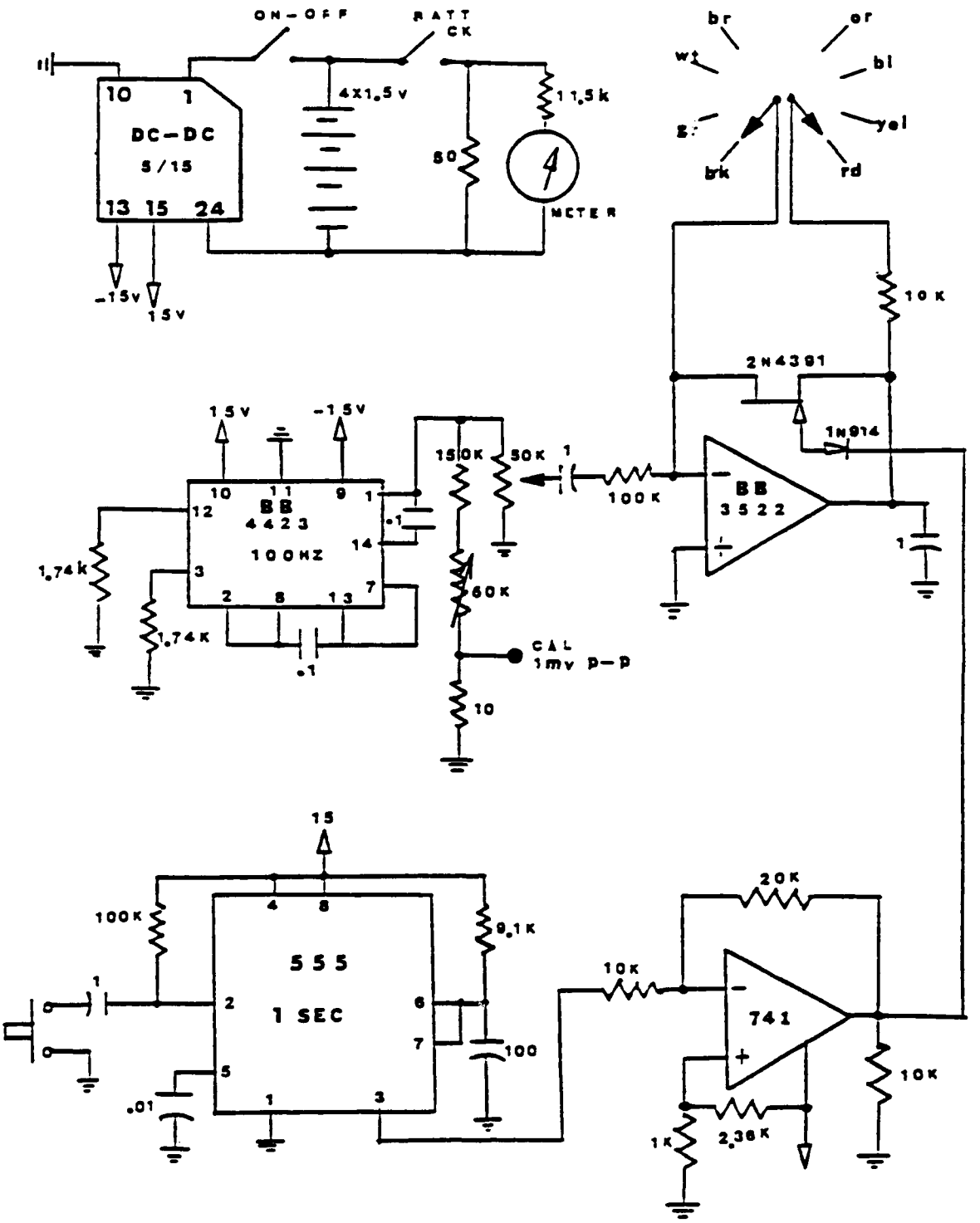

Figure 17. Schematic of the Prototype Lead Locator. Constant current of 100 Hz for 1 s to 1 of 4 leads.

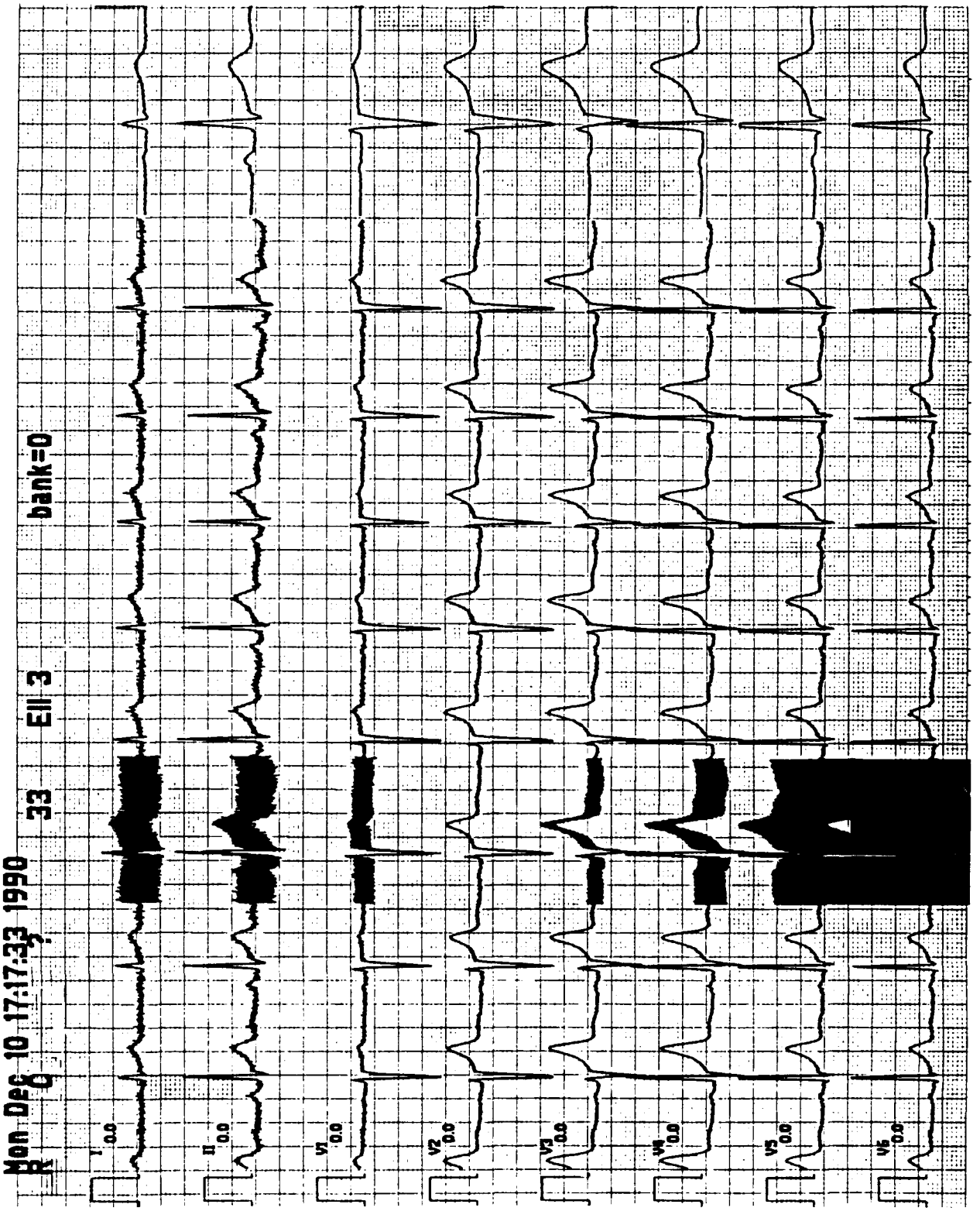

Figure 18. A 10 s epoch of the 30SL ECG, bank 0, with the 1 s current stimulation applied to a right-left, mid-axillary lead at the transverse level of the xiphoid.

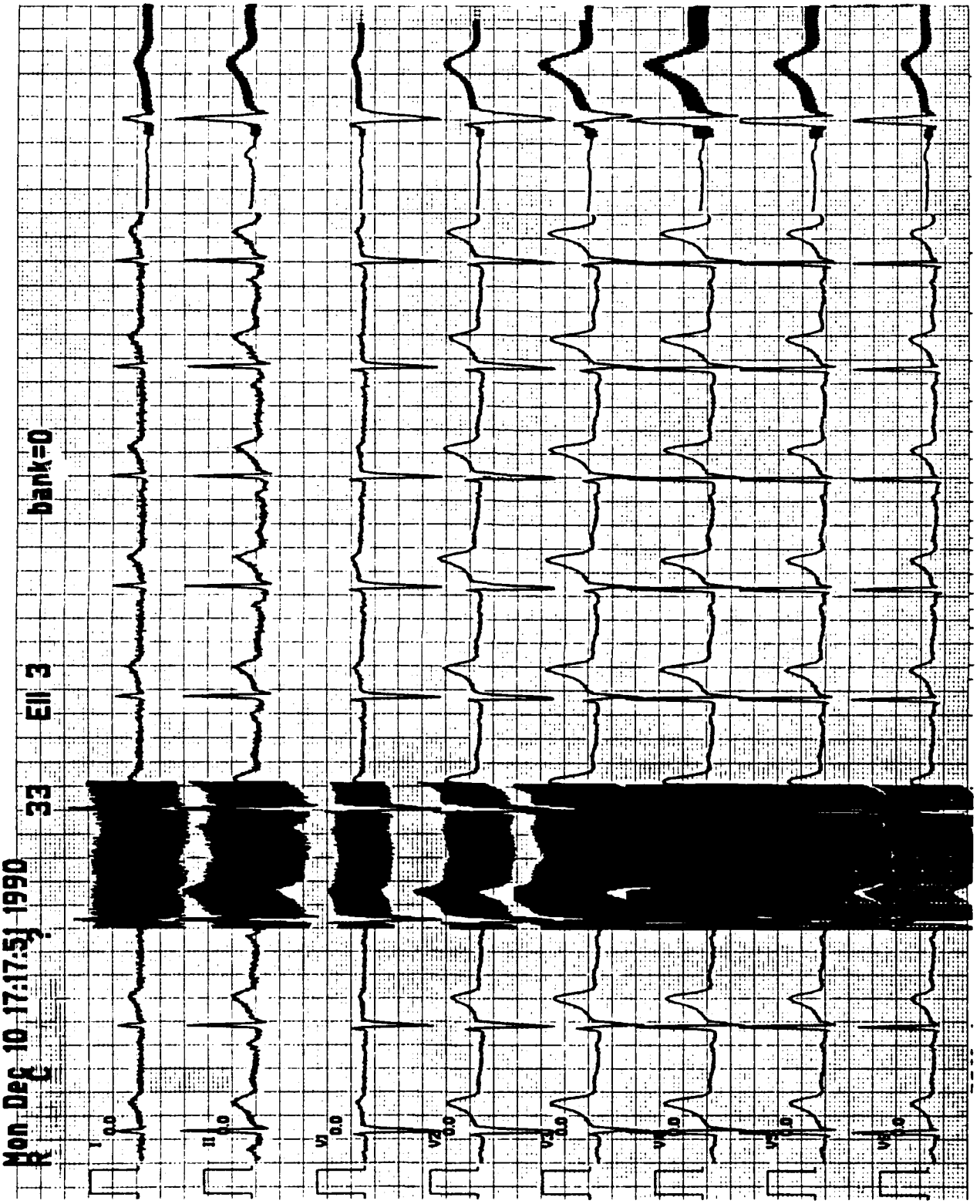

Figure 19. A 10 s epoch of the 30SL ECG, bank 0, with the current stimulation applied to a vertical lead at the left midclavicle and a point in the midclavicular line at the level of the xiphoid.

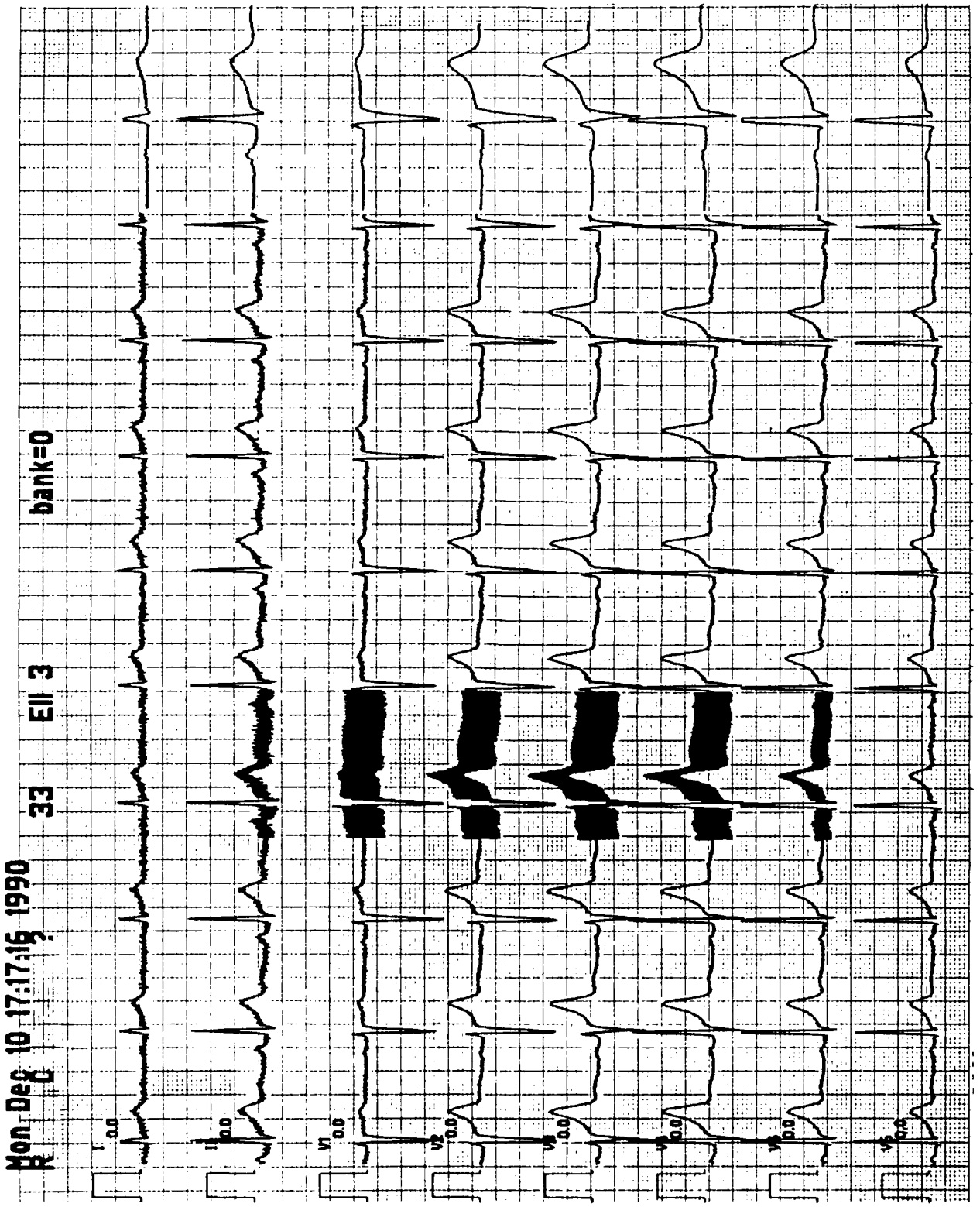

Figure 20. A 10 s epoch of the 30SL ECG, bank 0, with the 1 sec. current stimulation applied to an anterior-posterior lead in the midline at the transverse level of the xiphoid.

produced by a particular set of sites. As seen in the 3 tracings, right angle leads on the chest do not always produce orthogonal signals in the ECG leads. The present prototype lead locator will be used in a search for a set of well defined chest lead locations with signal separation in the 30 ECG leads, possibly up to 4 oblique leads.

Safety Report for Prototype Lead Locator.

The safety concerns regarding the use of the Lead Locator on humans fall into 2 categories: the normal functioning of the device as designed, and the worst-case failure analysis.

Under normal operating conditions the device maintains a constant current amplitude of 10 μa at a frequency of 100 Hz for 1 s. This injected current will remain constant for an electrode lead with an impedance between zero and 15 kohms, if the electrode impedance increases beyond 15 kohms the output current will decrease linearly. The literature (38-41) on the effects and hazards of currents applied to the chest surface of humans sets a nominal starting value of 1,000 μa for perception and discusses effects for currents beyond this level. There is no evidence that currents below 500 μa across the chest produce any risk or discomfort. The Lead Locator current is 100 times less and of no consequence when applied across the chest. The Lead Locator current should not be injected across chest leads if an intracardiac catheter is in place or the patient has a pacemaker, since 10 μa is considered the limit (42) for any ground loop currents or extraneous devices. Since the Lead Locator is isolated by four 1.5 v size "D" batteries, no ground loops are present; however, if one of the Lead Locator connections is to the catheter and the other to the chest then 10 μa would be applied directly to the heart.

Worst-Case Failure Mode.

The Lead Locator circuit design includes a DC/DC converter from 5 v to 15 v. A series resistor in the patient output lead of 10 kohms limits the injected current to 1.5 ma if a component failure should result in 15 v being applied to the output circuit. This level of DC current is slightly above the 1 ma level set for the threshold of perception, hence some patients might feel a tingling sensation at the electrode - skin interface. Again, this level of current is below the 5 ma range set as an acceptable safe level (39,43). A worst-case failure of this type could have severe effects if one of the leads were connected directly to an intra-heart catheter since 1.5 ma is well beyond the 10 μa limit. A warning is placed on the device:

DO NOT USE IN THE PRESENCE OF AN INTRA-CARDIAC CATHETER OR PACEMAKER!

ACKNOWLEDGMENT

The authors would like to give special acknowledgment to Javed Ahmed, M.D., for his dedicated effort and assistance in reviewing the data and in the preparation of this report.

REFERENCES

1. Einthoven, W., Fahr, G., and De Waart, A. Uber die Richtung und die Manifest Grosse der Potientelschwankungen im Menschlichen Herzen und uber den Infruss der Herzlage auf die Form des Elektrokardiogramms. Pflugers Arch. Ges. Physiol. 150:275, 1913.

2. Lewis, T. The Spread of the Excitatory Process in the Vertebrate Heart. Phil. Tr. Roy. Soc. Lond. 207:221, 1916.

3. Scher, A.M., Young, A.C., Malmgren, A.L., and Paton, R.R. Spread of the Electrical Activity in the Mammalian Ventricle. Circ. Res. 1:539, 1953.

4. Scher, A.M. and Young, A.C. Ventricular Depolarization and the Genesis of the QRS: Ann. N.Y. Acad. Sci. 65:768, 1957.

5. Durrer, D. and Van der Tweel, L.H. Excitation of the Left Ventricular Wall of the Dog and Goat. Ann. N.Y. Acad. Sci. 65:13, 1954.

6. Durrer, D., Van Dam, R.T., Freud, G.E., Janse, M.J., Meijler, F.L., and Arzbaecher, R.C. Total Excitation of the Isolated Human Heart. Circ. 41:899, 1970.

7. Selvester, R.H., Kirk, W.L., and Pearson, R.B. Propagation Velocities and Voltage Magnitudes in Local Segments of Myocardium. Circ. Res. 27(4):619, 1970.

8. Selvester, R.H., Kalaba, R., Kagiwada, H., Collier, C.R., and Bellman, R.: Simulated myocardial infarction with a mathematical model of the heart containing distance and boundry effects: Vectorcardiography 1965. I Hoffman, Ed. Amsterdam, NETHERLANDS: North Holland Publishing Co., 1966, pg. 403.

9. Selvester, R.H., Kalaba, R., Collier, C.R., Bellman, R., and Kagiwada, R. A Digital Computer Model of the Vectorcardiogram with Distance and Boundry Effects: Simulated Myocardial Infarction. Am Heart J 74:792, 1967.

10. Selvester, R.H. and Sanmarco, M.E. Infarct Size in Hi-Gain, Hi-Fidelity Serial VCGs and Serial Ventriculograms in Patients with Proven Coronary Artery Disease. Proceedings of the 4th World Congress on Electrocardiography, 1978.

11. Harumi, K., Burgess, M.J., and Abildskov, J.A. A Theoretic Model of the T Wave. Circ 34:657, 1966.

12. Thiry, P.S. and Rosenberg, R.M. On Electrophysiological Activity of the Normal Heart. J Franklin Inst 297:377, 1974.

13. Miller, W.T., III, and Geselowitz, D.B. Simulation Studies of the Electrocardiogram. I. The Normal Heart. II. Ischemia and Infarction. Circ Res 43:301, 1978.

14. Miller, W.T., III, and Geselowitz, D.B. Simulation Studies of the Electrocardiogram. II. Ischemia and Infarction. Circ Res 43(2):315, 1978.

15. Selvester, R.H., Solomon, J.C., and Gillespie, T.L. Digital Computer Model of a Total Body ECG Surface Map: An Adult Male Torso Simulation with Lungs. Circ 38:684, 1968.

16. Solomon, J.C. and Selvester, R.H. Current Dipole Moment Density of the Heart. Am Heart J 81(3):351, 1971.

17. Solomon, J.C. and Selvester, R.H. Simulation of Measured Activation Sequence in the Human Heart. Am Heart J 85(4):518, 1973.

18. Selvester, R.H., Wagner, J.O., and Rubin, H.B.: Quantitation of Myocardial Infarct Size and Location by Electrocardiogram and Vectorcardiogram. Quantitation in Cardiology. Snellen, Hemker, Hugenholtz and Van Bremmel, eds., Leiden University Press, 31, 1972.

19. Selvester, R.H., Sanmarco, M.E., Solomon, J.C., and Wagner, G.S.: Methods of Determining Infarct Size, ECG: QRS Change. Myocardial Infarction: Measurement and Intervention. Wagner, G.S., Ed., Martinus Nijhoff, The Hague, Boston, London, 1982, pg 23.

20. Palmeri, S.T., Harrison, D.G., Cobb, F.R., Morris, K.G. Harrell, F.E., Ideker, R.E., Selvester, R.H., and Wagner, G.S. A QRS Scoring System for Assessing Left Ventricular Function after Myocardial Infarction. N. Eng J Med 306(1):4, 1982.

21. Wagner, G.S., Freye, C.H., Palmeri, S.T., Roark, S.F., Stack, B.A., Ideker, R.E., Harrell, F.E., and Selvester, R.H. Evaluation of a QRS Scoring System for Estimating Myocardial Infarct Size. I. Specificity and Observer Agreement. Circ 65:342, 1982.

22. Ideker, R.E., Wagner, G.S., Ruth, W.K., Alonso, D.R., Bishop, S.P., Bloor, C.M., Fallon, J.T., Gottlieb, G.J., Hackel, D.B., Phillips, H.R., Reimer, K.A., Roark, S.F., Rogers, W.J., Savage, R.M., White, R.D., and Selvester, R.H. Evaluation of a QRS Scoring System for Estimating Myocardial Infarct Size. II. Correlation with Quantitative Anatomic Findings for Anterior Infarcts. Am J Cardiol 49:1604, 1982.

23. Roark, S.F., Ideker, R.E., Wagner, G.S., Alonso, D.R., Bishop, S.P., Bloor, C.M., Bramlet, D.A., Edwards, J.E., Fallon, J.T., Gottlieb, G.J., Hackel, D.B., Phillips, H.R., Reimer, K.A., Rogers, W.J., Ruth, W.K., Savage, R.M., White, R.D., and Selvester, R.H. Evaluation of a QRS Scoring System for Estimating Myocardial Infarct Size. III. Correlation with Quantitative Anatomic Findings for Inferior Infarcts. Am J Cardiol 51:382, 1983.

24. Ward, R.M., White, R.D., Ideker, R.E., Hindman, N.B., Alonso, D.R., Bishop, S.P., Bloor, C.M., Fallon, J.T., Gottlieb, G.J., Hackel, D.B., Hutchins, G.M., Phillips, H.R., Reimer, K.A., Roark, S.F., Rochlani, S.P., Rogers, W.J., Ruth, W.K., Savage, R.M., Weiss, J.L., Selvester, R.H., and Wagner, G.S. Evaluation of a QRS Scoring System for Estimating Myocardial Infarct Size. IV. Correlation with Quantitative Anatomic Findings for Posterolateral Infarcts. Am J Cardiol 53:706, 1984.

25. Solomon, J.C., Selvester, R.H., and Tolan, G.D.: An Enhanced Forward Model of the Heart. Engineering Foundation Conference. Computerized Interpretation of the Electrocardiogram XI. Bailey, J.J., Ed. Engineering Foundation, New York, 1986, pg 146.

26. Selvester, R.H., Solomon, J.C., and Tolan, G.D. Fine Grid Computer Simulation of QRS-T and Criteria for the Quantitation of Regional Ischemia. Computerized Interpretation of the ECG XII, Proceedings Engineering Foundation Conferences, Kligfield, P., Bailey. J.J. Eds., J Electrocardiology 21:Supplement I. 1987.

27. Kornreich, F., Rautaharju, P.M., Warren, J.W., Block, P., and Dramaix, M.: The Contribution of Body Surface Potential Maps to Optimal Lead Sets. Computerized Interpretation of the ECG IX, Proceedings of the Engineering Foundation Conference. Selvester, R., Ed. Engineering Foundation New York, 1983.

28. Kornreich, F., Montague, T.J., Rautaharju, P.M., Kavadias, M., Horacek, M.B., and Taccardi, B. Multigroup Diagnosis of Body Surface Potential Maps. Journal of Electrocardiology, Volume 22: Supplement, 1989.

29. Kornreich, F., Montague, T.J., Rautaharju, P.M. et al. Identification of Best Electrocardiographic Leads for Diagnosing Anterior and Inferior Myocardial Infarction by Statistical Analysis of Body Surface Potential Maps. Am J Cardiol 58:863, 1986.

30. Allred, E.N., Blecker, R.E., Chaitman, R.B., Dahms, T.E., Gotlieb, S.O., Hackney, J.D., Pagano, M., Selvester, R.H., Walden, S.M., and Warren, J. Short-Term Effects of Carbon Monoxide Exposure on the Exercise Performance of Subjects with Coronary Artery Disease. N Eng J Med 321:1426-1432, 1989.

31. Selvester, R.H. and Solomon, J.C. Optimal ECG Electrode Sites and Criteria for Detection of Asymtomatic Coronary Artery Disease at Rest and with Exercise. USAFSAM-TR-85-47, December 1985.

32. Ellestad, M.H. Stress Testing: Principles and Practice, 3rd Edition. Philadelphia, PA: F. A. Davis Co., 1986.

33. Mason, R.E. and Likar, I. A New System of Multiple-Lead Exercise Electrocardiography. Am Heart J 71:196-205, 1966.

34. Selvester, R.H., and Gillespie, T.L. Simulated ECG Body Surface Map's Sensitivity to Local Segments of Myocardium in Body Surface Mapping of Cardiac Fields. Rush, S., and Lepeschkin, E., Eds. Advanced Cardiol. 10:120-125, Karger, Basel, 1974.

35. Selvester, R.H., Solomon, J.C., and Pearson, R.B.: ECG Body Surface Map Criteria for Quantitating Infarct, as Derived from Computer Simulations. 3rd International Symposium on Body Surface Mapping. van Dam, R.T., and van Oosterom, A., Eds. Boston, MA: Martinus Nijhoff Publishing Co., 1985.

36. Madrid, W.L., Sanmarco, M.E., Gaarder, T.G., and Selvester, R.H. Circumflex Occlusion and Posterior Myocardial Infarction: Diagnostic Criteria and Automated ECG Analysis Programs: Computerized Interpretation of the ECG XI, Proceedings Engineering Foundation Conferences. Bailey. J.J. Ed. Engineering Foundation, New York, 1986.

37. Selvester, R.H., Wagner, G.S., and Ideker, R.E.: Myocardial Infarction: Comprehensive Electrocardiology. Macfarlane, P.W. and Lawrie, T.D., Eds. New York: Pergamon Press, 1989. pgs. 565-629.

38. Bruner, John M.R. Hazards of Electrical Apparatus. Anesthesiology 28(2): 122-128 March-April 1967.

39. Green, H.L., Breneman, G.M., Goldberg, S.J., Harken, D.E., Hieb, G.E., Kosowsky, B., Parker, B., Rinaldo, J.A., Webb, G.N., and Nobel, J.J. Electronic Equipment in Critical Care Areas. Part II:The Electrical Environment. Circ, 44:A-23, 1971.

40. Starmer, C.F., Whalen, R.E., and McIntosh, H.D. Hazards of Electric Shock in Cardiology. Am J of Cardiol 14:537-546, 1964.

41. Cromwell, L., Weibell, F.J., Pfeiffer, E.A., and Usselman, L.B.: Biomedical Instrumentation and Measurements. Englewood Cliffs, New Jersey: Prentice-Hall Publishing Co., 1973, pg. 374.

42. Whalen, R.E., Starmer, C.F., and McIntosh, H.D. Electrical Hazards Associated With Cardiac Pacemaking. Ann N Y Acad Sci, III:921-931.

43. Kossmann, C.E., Brody, D.A., Burch, G.E., Hecht, H.H., Johnston, F.D., Kay, C., Lepeschkin, E., Pipberger, H.V., Baule, G., Berson, A.S., Briller, S.A., Geselowitz, D.B., Horan, L.G., and Schmitt, O.H. Recommendations for Standardization of Leads and of Specifications for Instruments in Electrocardiography and Vectorcardiography. Circ, 35:588, 1967.

APPENDIX

Technical Report

Fine Grid Computer Simulation of QRS-T and Criteria for the Quantitation of Regional Ischemia

BY RONALD H. SELVESTER, JOSEPH C. SOLOMON AND GIL D. TOLAN

SUMMARY

A comprehensive fine grid simulation of excitation and recovery (QRS-T), realistic cardiac and torso anatomy, and electrophysiologic properties has been developed that produces a total body surface electrocardiogram (ECG) as output. The simulation leads to the specific hypothesis that additional leads on the upper and lower torso, and on the back, are required to optimize the quantitation and localization of regional ischemia and infarction. Criteria in the STT portion of the ECG for quantitating the severity of the ischemia were developed and presented. The combination of the leads in which the STT changes occur and the severity of the STT change provide a testable set of hypotheses for predicting the severity of ischemia, the probable coronary perfusion bed involved, the severity of the perfusion defect, and the severity of the proximal coronary obstruction.

The computer simulation of the human total body surface ECG developed by us over the past several years was constructed from measured torso anatomy, resistivities, and electrophysiology.[1-3] A digital computer simulation of the excitation wave based on the Huygens principle of wave construction using a distributed dipole model of electromotive surface,[4,5] and measured normal heart and infarct geometry, was developed at a 1 cu mm grid resolution. The electrical activity from the fine grain local surface was then projected to the centroid of 20 regional cardiac generators imbedded in a realistic inhomogeneous torso that included intracardiac blood mass, lungs, muscle, and an adult male torso boundary. Transfer impedances between the regional sources and some 1300 torso locations were generated by the Gelernter-Swihart solution.[3] Combining the regional cardiac equivalent generator output with the transfer impedances yielded a mathematical-physical simulation containing all the first order variables known to influence the QRS of the human ECG. A series of numerical experiments with the model led to a set of vectorcardiographic (VCG) and ECG criteria and a QRS point score (1 point = 3% of the left ventricle) for quantitating myocardial infarct size in all locations of the heart.[6,7] Working with the Duke group over the next several years, the QRS infarct size score was validated in a series of classic pathoanatomic studies[8-12] that have been reported at a number of previous meetings of this society.

Harumi, Burgess and Abildskov, building on the ventricular gradient notions of Wilson, were the first to develop a model of the T wave.[13] Thiry and Rosenberg later developed a multiple dipole simulation of repolarization in three dimensions.[14] Miller and Geselowitz reported a 4 mm grid heart model in a homogeneous torso in which they manually entered changes in excitation and recovery parameters.[15] These models successfully simulated typical 12-lead ECG changes of ischemia, injury, and infarction by incorporating action potential waveshapes and distributions for these conditions typical of those measured in the laboratory. In order to improve the resolution for infarction and to expedite numerical experiments with the model, we have automated the grid heart model of Miller and Geselowitz in a 1 mm grid heart in an inhomogeneous torso. This results in a comprehensive simulation of excitation and recovery, i.e., QRS-T.

Last year in Santa Barbara Joe Solomon reported[16] on early results of automating the incorporation of individual action potential wave forms into each of the 1 cu mm "cells" of this simulation. We have now developed the high resolution color graphics programs for displaying the entire depo-

From the University of Southern California, Rancho Los Amigos Campus, Downey, CA and USAF School of Aerospace Medicine, Brooks Air Force Base, TX.

Reprints requests to: Ronald H. Selvester, M.D., Med Science Bldg, Room 26, Rancho Los Amigos Med Center, 7601 E. Imperial Hwy, Downey, CA 90242.

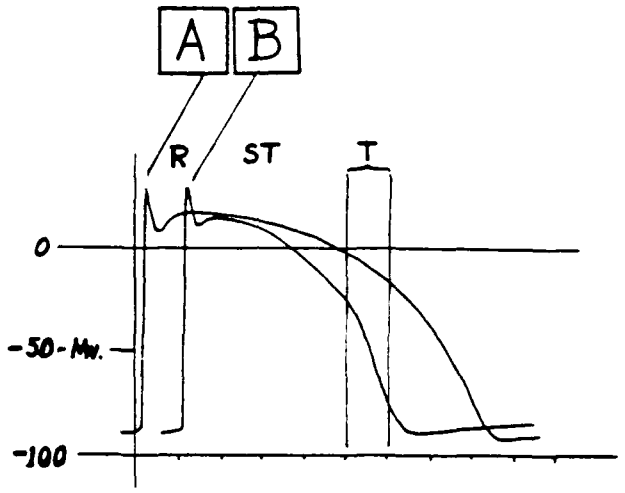

Fig. 1. Endocardial (A) and epicardial (B) myocardial action potentials (MAPs) that are typical of those introduced into the simulation are shown here. Note that the duration of the endocardial MAP is much longer.

larization-repolarization cycle on a set of cross sections of the heart seen in a 3D perspective. The complete QRS-T sequence can be visually displayed for a normal heart, or for one with any combination of regional ischemia or infarction. The complete body surface ECG is the usual output of the program and subsets of this map such as the 12-lead ECG and any VCG lead system can be plotted for each of the above combinations. It is the purpose of this paper to present typical examples of recent color graphic and 12-lead ECG outputs and to propose criteria based on the complete QRS-T simulation for localizing and quantitating ischemia (in addition in infarction) in each of the major coronary artery distributions.

METHODS AND RESULTS

Our method of constructing the repolarization generator makes use of an equation containing three arbitrary parameters that assume values which permit the time course of the myocardial action potentials (MAPs) to be approximated. The three parameters characterizing the MAP are the recovery potential, rate of repolarization, and the functional refractory period. With these three parameters and four constants (initial resting potential, time to depolarize, peak depolarization potential, and a time constant which represents the time for the local region to reach equilibrium), each discrete point within the myocardium can be represented by a

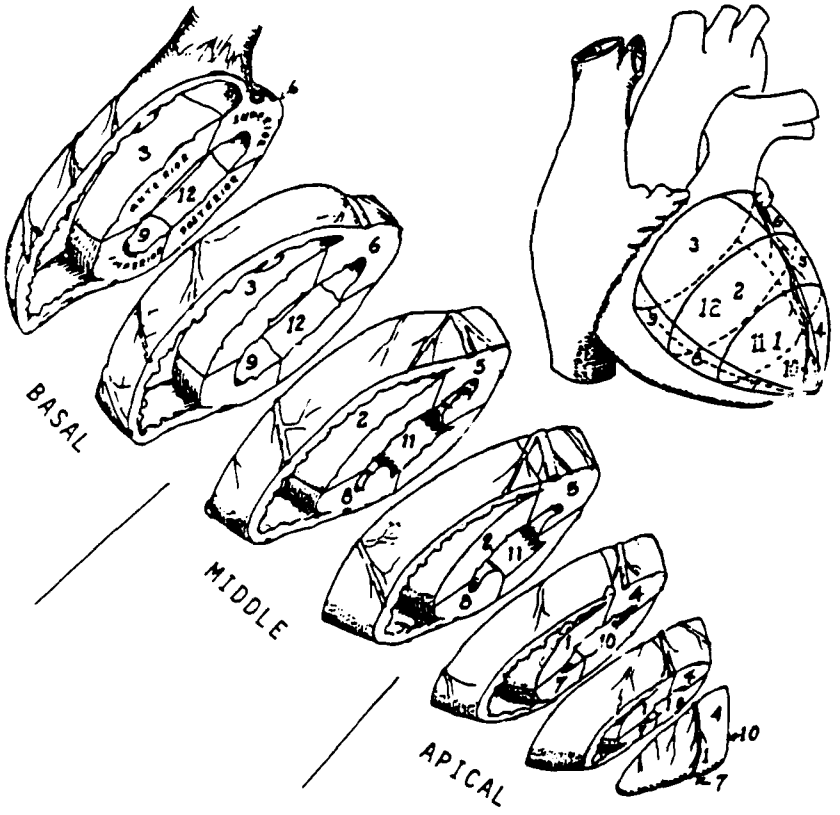

Fig. 2. A 12-segment subdivision of the left ventricle is shown in the right upper part of this figure. The typical four circumferential quadrant subdivision is shown along with three apex to base segments in each wall that we have used in developing criteria for localizing and sizing myocardial infarcts. The "bread loaf" cross sections shown are presented here mainly for orientation purposes. They are viewed from the same perspective as the computer graphic presentations of Figs. 3A and 4A.

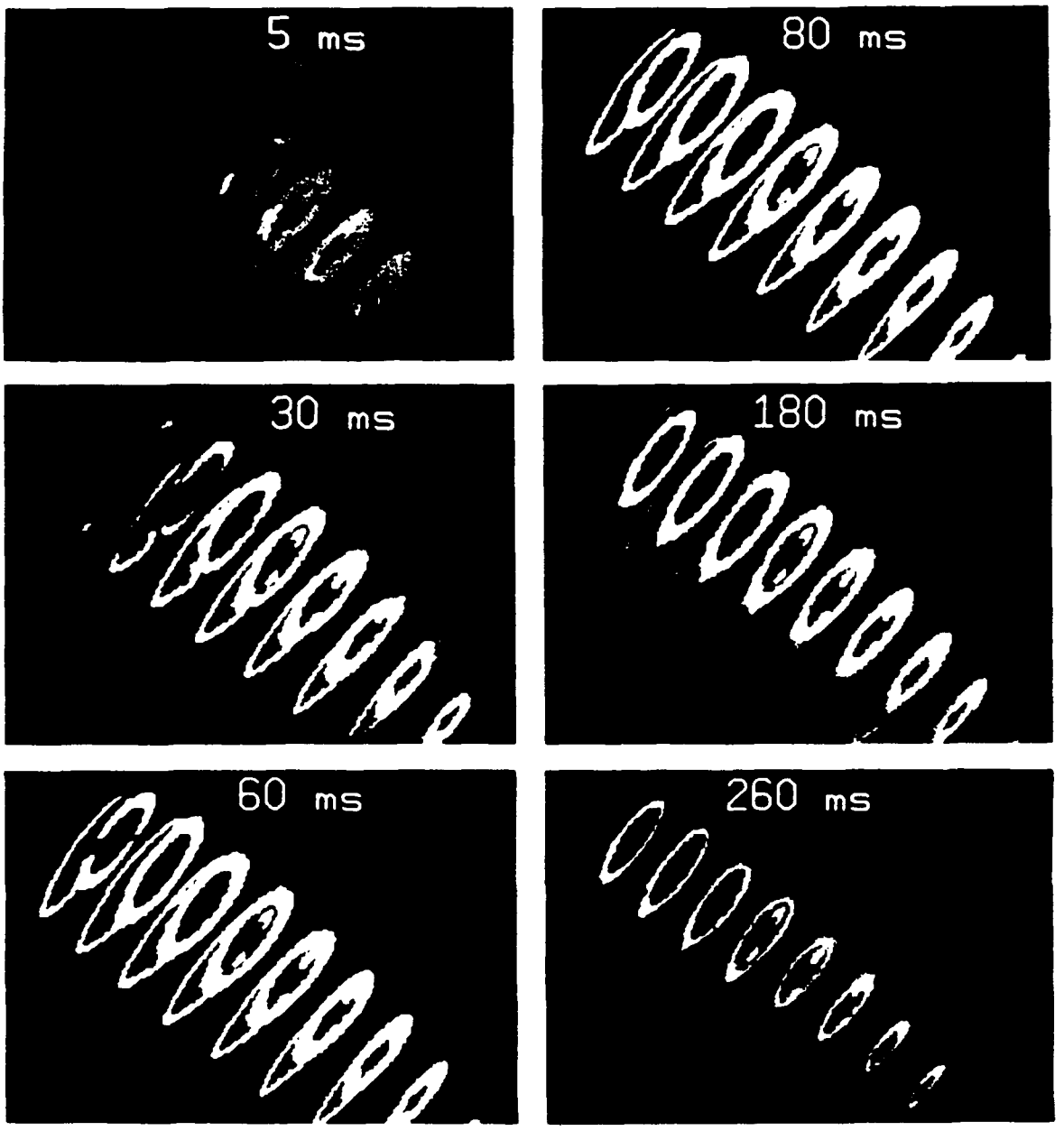

Fig. 3A. Black and white renditions of the colorgraphic output of the computer simulation of a normal excitation recovery sequence is presented here. The cross sections are selected from the complete set and are at 10 mm intervals. Each is at right angles to the long axis of the left ventricle. Thus each section as viewed from the anterior perspective reveals its underside (see Fig. 2 for orientation). Resting myocardium is dark on these sections. Excitation begins on the left septal surface in the mid portion near the junction with the apical third as shown and progresses rapidly to the endocardium of the left ventricle by 30 ms. It propagates from endocardium to epicardium. The active region at the excitation front is limited to about 3 mm. Recovery is a slower process and is more distributed. The myocardial action potential durations are adjusted in the simulation so that recovery procedes from epicardium to endocardium around the perimeter of the left ventricle. Recovery is just underway at 180 ms, has proceded to the midwall of the left ventricle by 260 ms, and is approaching the subendocardium, the last region to be repolarized.

unique waveform (see Fig. 1). These parameters are found by a table look up that incorporates the endocardium to epicardium gradient in MAP durations and refractory periods as well as the apex to base gradient. A separate table contains the four constants described above that are mainly influenced by injury, ischemia, and the electrolyte milieu of the active cells. This allows for the specifi-

cation of local areas of the injury/ischemia/infarction by their effects on local MAPs.

Individual MAPs from each 1 cu mm "cell" were then projected to the 20 regional equivalent cardiac generators and combined with a Gelernter-Swihart solution for the heart-to-chest transfer impedances. A typical segment subdivision of the left ventricle is shown in Fig. 2. Also shown are typical "bread loaf" cross sections of the heart seen in the same perspective as that of the usual computer colorgraphic output of heart cross sections depicting excitation and recovery. Combining the generator and transfer impedances yielded a mathematical-physical simulation containing arbitrary parameters that were adjusted such that numerically computed body surface T-wave distributions were made to agree with those measured on human subjects. First the model was adjusted to fit a normal 12-lead ECG. Illustrative frames from these simulations of excitation/recovery are shown in Figs. 3A, B along with the simulated normal ECG. A large anterior infarct was then simulated using the quantitative planometric pathology of such a lesion from the Duke validation studies described in the introduction. The details of the infarct that was introduced are shown in Fig. 4A. In this case no alterations to simulate ischemia in the border zone or other areas were introduced. Fig. 4B is the 12-lead ECG from the simulation which shows the typical changes seen clinically in the chronic phase of such large anterior infarcts.

The potential role of resistivity changes in the volume conductor that might occur with exercise were next examined. A small current was introduced after the S wave at one electrode and voltages were measured at each of 160 different electrodes. Change in voltage was assessed before and during each phase of a maximal exercise test. Presentation of the details are outside the scope of this short paper but in summary it was found that the changes in torso resistivities with maximal exercise were within the noise level on the signal processed ECG data from the same studies. It was concluded therefore that the heart-to-torso transfer impedances could be assumed to be stable from rest to exercise.

DISCUSSION

In previous studies reported at earlier meetings of this conference a minimum set of chest electrodes was selected which optimized the sensitivity of the model to regional infarct with respect to ECG waveform changes. In simulated normal and in subendocardial ischemia, the QRS and STT vectors from each of the local myocardial regions were essentially parallel to each other. It follows that if electrode sites are chosen that are relatively specific for each local region the amplitude of both QRS and STT can be normalized to the average voltage (i.e., 1.3 mv) in the reference lead V5 as done by Hollenberg.[17] When this is done, the same amplitude of local STT changes in each of the surface leads shown in Fig. 5 now represents approximately the same degree and extent of regional ischemia. It can be assumed also that a time integral of the ST (and/or T) with modifications that include time in recovery, etc., as per the Hollenberg method would further improve both sensitivity and specificity of the method.

One of the major strengths of a simulation constructed from anatomic and electrophysiology information is that it can be used to generate testable hypotheses regarding the process simulated. We are now at that stage in the model development. The following criteria and lead locations are proposed for exercise testing done before coronary angiography. This would be particularly applicable to populations of apparently healthy subjects, such as business executives and commercial or Air Force pilots, who are undergoing extensive testing including coronary angiography because of abnormalities suggesting a high risk of coronary disease in a battery of screening tests.

Recommended Lead Locations on the Thorax

Twenty simultaneous leads; alternatively, 3 sets of 8 simultaneous leads, each set including the same 2 selectable leads, i.e., III and V5. The leads are recorded as follows:

A. Limb leads: LA and RA on clavicles, LL and RL on the left and right lower rib cage in the midaxillary line (MAL). Two limb leads are simultaneous, the other four are computed.
B. 18 simultaneous precordial and back leads located as follows:
   1. Six standard precordial leads (V1–V6), records the left anterior descending (LAD) area, mainly anteroseptal wall and the apex (other regions poorly shown).
   2. Upper chest leads V3(ICS3) and V5(ICS3) in 3rd intercostal space: Records LAD/DIAG area (anterosuperior wall).
   3. Right and lower chest leads; V1(ICS2), V4R and 4 leads at the level of the 7th ICS in the MAL V4R(ICS7), VPXR (*ParaXiphoid* rt ICS7), VPX(ICS7), and V4(ICS7). Records right coronary and posterior descending

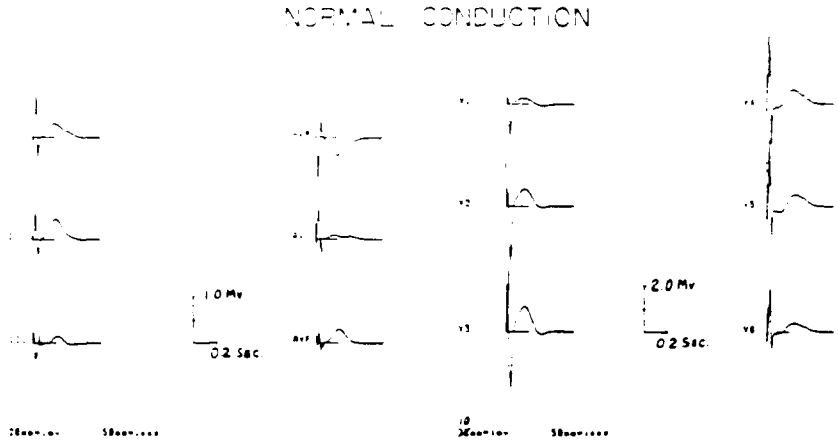

Fig. 3B. This figure is the 12-lead ECG from the simulation in Fig. 3A.

(RCA-PDA) arterial area (right ventricle and inferior wall of both ventricles).

4. Back leads V8, VMB (*M*id *B*ack), V8R, and VSR (*S*capula, *R*ight acromion in the mid clavicular line). Records left circumflex arterial area (posterolateral wall).

Note: Optimally these can be recorded as a 20 simultaneous lead set, and processed in line. The relationship of lead locations and individual myocardial segments is shown in Fig. 5. Alternatively, 3 sets of 8 simultaneous leads can be recorded in 20-second blocks with switching between sets, leads III and V5 (or any two leads) being monitored continuously. Each set can thus be signal processed with a mean or median beat recorded each minute of exercise.

Criteria for Quantitation of Regional Ischemia

The following are proposed criteria that we believe are ready for rigorous testing as to both specificity and sensitivity for regional subendocardial ischemia in each of the main coronary artery distributions:

I. Simple measurements of ST segments at J, and ST 60 ms, 80 ms after J produced by stress atrial pacing, maximal treadmill exercise, etc. All ST measurements to be normalized to an R amplitude in that lead of 1.3 mv.

A. General—severity of **subendocardial ischemia** in any location or lead set (normalized voltages); criteria for J and ST60 as follows:

	J and ST60 depressed and ST flat or downsloping and	J and ST60 depressed and or ST upsloping and
Borderline:	depressed ≥ 0.075 mv	depressed ≥ 0.15 mv
Probable:	depressed ≥ 0.1 mv	depressed ≥ 0.175 mv
Mild but def.:	depressed ≥ 0.15 mv	depressed ≥ 0.2 mv
Moderate:	depressed ≥ 0.2 mv	depressed ≥ 0.25 mv
Severe:	depressed ≥ 0.3 mv	depressed ≥ 0.35 mv

B. Specific—Predicted local segment, and coronary artery diseased; the severity in any location is based on the normalized ST criteria above; the location of the probable risk area and coronary artery is based on the local torso leads in which change occurs as follows:
1-Vessel disease, abnormal ST change in following leads:
- ●LAD distal to the Diagonal: Leads V3–V5 and V5(ICS7).
- ●Diagonal: Leads I, AVL, V3(ICS3), V5(ICS3), and V6.
- ●LAD proximal to the Diagonal: V2 + any 2 or more of the above.

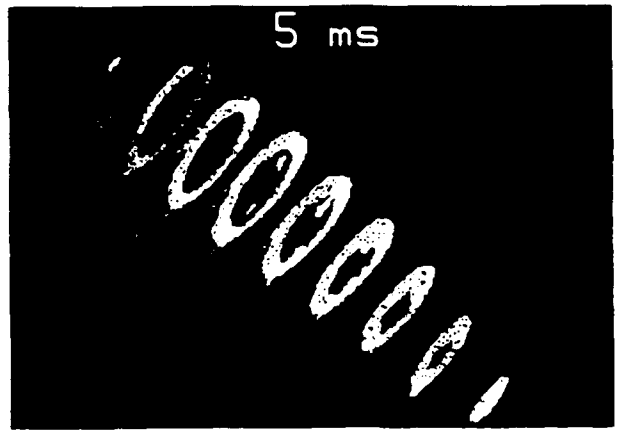

Fig. 4A. A large anterior infarct is shown in stippled white in this figure. It was transferred from photographs (and histological slides) of "bread loaf" pathoanatomic cross sections of a human infarct provided by R. Ideker, M.D. of Duke University Medical Center of Durham, NC.

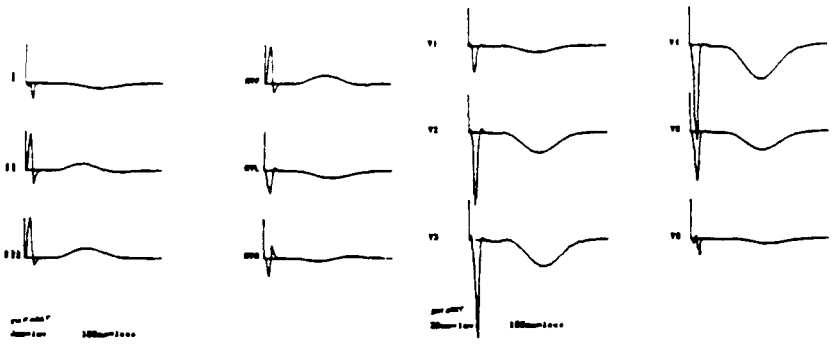

Fig. 4B. This is the 12-lead ECG resulting from the infarct simulation in Fig. 4A. No ischemia was introduced into the model in this case. The T wave changes in this ECG are the result of the simple absence of cardiac generators over the large area of the infarct during both excitation and recovery.

- ●LCX: Leads V8, VMB, V8R, and VSR (Scapula, Rt Acromion, MCL)*.
- ●PDA/RCA: ICS7 Leads V4R, VPXR, and VPX*.

*Note: involvement of left right (apical) leads I, V5, V6, and V5(ICS7) in addition to the posterior (LCX), or inferior (PDA/RCA) leads is a marker of more extensive area of ischemia although still 1-vessel disease.

2-Vessel disease:

- ●Changes of LAD + LCX, LAD + PDA/RCA, and LCX + PDA/RCA as defined above under 1-vessel disease.

  Note: the severity may differ in each arterial area at risk.

3-Vessel disease:

- ●Changes of LAD + LCX + PDA/RCA as defined under 1-vessel disease.

  Note: as with 2-vessel disease, the severity may differ in each arterial area at risk.

4-Vessel, i.e., Left Main disease:

- ●Early onset of moderate to severe ischemia in Prox. LAD + LCX (usually also + PDA/RCA) especially if associated with a 20 mm Hg or more drop in systolic BP.

Note: in this case the severity in both the LAD and LCX risk areas should be equivalent but the severity in the PDA/RCA risk area may differ.

II. Time integral methods of evaluating STT change

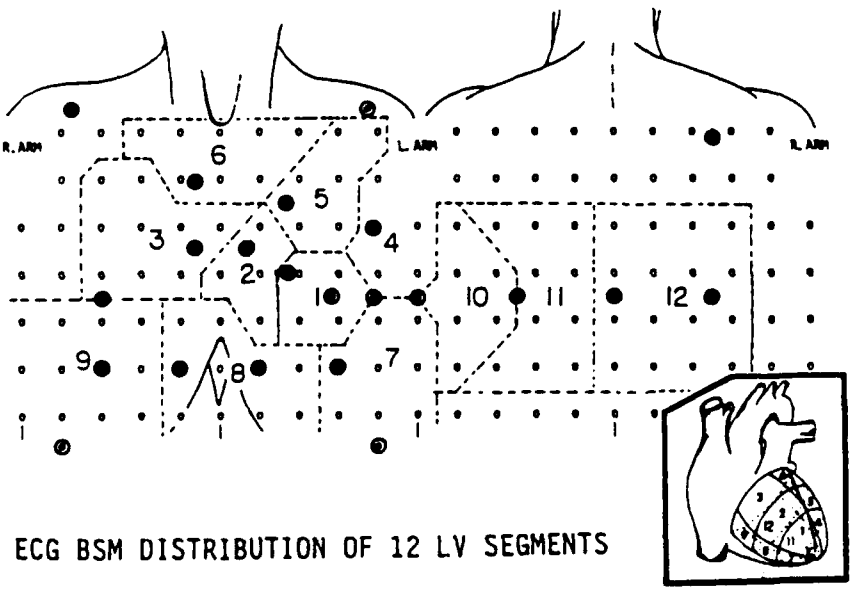

Fig. 5. Recommendations for the location of 22 electrode sites for the recording of the 20 simultaneous stress ECG leads as discussed in the text. The projection of the 12 left ventricular segments (shown in the insert) to the body surface is also indicated here. The location of 22 electrode sites from which 20 independent leads are recorded is shown here. Two limb leads are recorded from right and left arm electrodes at the distal end of each clavicle and from the left leg electrode on the left lower anterior rib cage. The right leg reference electrode is placed on the right lower rib margin anteriorly. The four remaining standard limb leads are computed from these two. Besides the six standard precordial leads, extra leads are added as shown at the level of the 3rd, 5th, and 7th anterior intercostal spaces and on the back.

with stress: i.e., atrial pacing and maximal exercise testing etc. In each of the methods outlined below, the magnitude of the ST time integral (normalized to 1.3 mv in the specific lead) would be related to severity of regional ischemia, and the location on the torso of these changes would be predictive of the specific arterial risk area.

A. The time, J point ST integral method of Hollenberg with weighting factors for ST slope, sex, total time including ten minutes of recovery, maximum heart rate as a percent of age predicted, etc.
B. Time integral of the entire abnormal ST segment with and without the weighting factors listed above.
C. Time integral of the change from resting of the entire ST and T segment of repolarization with and without the weighting factors above.

Validation Studies

In the type of subjects who are apparently healthy but who have changing history, risk profile, blood chemistries, or ECG changes and who have stress test abnormalities or other indications for coronary angiography, those who have normal coronary arteries at angiography provide the normal controls for specificity studies. Those with definite exercise perfusion defects in one coronary distribution who have 70% or more narrowing of that coronary artery are the study population with which to validate the proposed criteria for localizing the risk area and quantitating the ischemia in the region. The specific criteria outlined earlier for quantitating ST segments, and the relating of these changes to the severity of coronary obstruction, will need to be adjusted for high specificity and optimal sensitivity based on the population they are being used in. In the low incidence, apparently healthy groups mentioned above, the specificity should be set at better than 95% for exercise testing using this lead set to be an effective screening tool in this population.

Some 20% of totally occluded coronary arteries are not associated with regional wall motion abnormalities at rest. About half of such patients in most series do not have perfusion defects or wall motion abnormalities with exercise. It follows from these data that a small subset of subjects in the validation study herein proposed will also have significant coronary disease but can be expected to have normal or borderline perfusion studies and ST segment change with exercise on multilead ECGs. One can postulate that the functional impairment in such cases would be minimal or insignificant, and that long term morbidity and mortality would be significantly better in this subset.

REFERENCES

1. Selvester, R H, Kalaba, R, Kagiwada, H, Collier, C R and Bellman, R: Simulated myocardial infarction with a mathematical model of the heart containing distance and boundary effects. *In* Vectorcardiography 1965. I Hoffman, Ed. North Holland Publishing Co, Amsterdam, 1966, p 403
2. Selvester, R H, Kalaba, R, Collier, C R, Bellman, R and Kagiwada, H: A digital computer model of the vectorcardiogram with distance and boundary effects: simulated myocardial infarction. Am Heart J 74:792, 1967
3. Selvester, R H, Solomon, J C and Gillespie, T L: Digital computer model of a total body ECG surface map. An adult male torso simulation with lungs. Circ 38:684, 1968
4. Solomon, J C and Selvester, R H: Simulation of measured activation sequence in the human heart. Am Heart J 85(4):518, 1973
5. Solomon, J C and Selvester, R H: Current dipole moment density of the heart. Am Heart J 81(3):351, 1971
6. Selvester, R H and Sanmarco, M E: Infarct size in hi-gain, hi-fidelity serial VCGs and serial ventriculograms in patients with proven coronary artery disease. Proceedings of the 4th World Congress on Electrocardiography, 1978
7. Selvester, R H, Sanmarco, M E, Solomon, J C and Wagner, G S: Methods of determining infarct size, ECG: QRS change. *In* Myocardial Infarction: Measurement and Intervention. Wagner G S, Ed. Martinus Nijhoff, The Hague, Boston, London, 1982, p 23
8. Palmeri, S T, Harrison, D G, Cobb, F R, Morris, K G, Harrell, F E, Ideker, R E, Selvester, R H and Wagner, G S: A QRS scoring system for assessing left ventricular function after myocardial infarction. N Engl J Med 306(1):4, 1982
9. Wagner, G S, Freye, C H, Palmeri, S T, Roark, S F, Stack, B A, Ideker, R E, Harrell, F E and Selvester, R H: Evaluation of a QRS scoring system for estimating myocardial infarct size. I. Specificity and observer agreement. Circ 65:342, 1982
10. Ideker, R E, Wagner, G S, Ruth, W K, Alonso, D R, Bishop, S P, Bloor, C M, Fallon, J T, Gottlieb, G J, Hackel, D B, Phillips, H R, Reimer, K A, Roark, S F, Rogers, W J, Savage, R M, White, R D and Selvester, R H: Evaluation of a QRS scoring system for estimating myocardial infarct size. II. Correlation with quantitative anatomic findings for anterior infarcts. Am J Cardiol 49:1604, 1982
11. Roark, S F, Ideker, R E, Wagner, G S, Alonso, D R, Bishop, S P, Bloor, C M, Bramlet, D A, Edwards, J E, Fallon, J T, Gottlieb, G J, Hackel, D B, Phillips, H R, Reimer, K A, Rogers, W J, Ruth, W K, Savage, R M, White, R D and Selvester, R

H: Evaluation of a QRS scoring system for estimating myocardial infarct size. III. Correlation with quantitative anatomic findings for inferior infarcts. Am J Cardiol 51:382, 1983

12. Ward, R M, White, R D, Ideker, R E, HIndman, N B, Alonso, D R, Bishop, S P, Bloor, C M, Fallon, J T, Gottlieb, G J, Hackel, D B, Hutchins, G M, Phillips, H R, Reimer, K A, Roark, S F, Rochlani, S P, Rogers, W J, Ruth, W K, Savage, R M, Weiss, J L, Selvester, R H and Wagner, G S: Evaluation of a QRS scoring system for estimating myocardial infarct size. IV. Correlation with quantitative anatomic findings for posterolateral infarcts. Am J Cardiol 53:706, 1984
13. Harumi, K, Burgess, M J and Abildskov, J A: A theoretic model of the T wave. Circ 34:657, 1966
14. Thiry, P S and Rosenberg, R M: On electrophysiological activity of the normal heart. J. Franklin Inst 297:377, 1974
15. Miller, W T, III and Geselowitz, D B: Simulation studies of the electrocardiogram. I. The normal heart. II. Ischemia and infarction. Circ Res 43:301, 1978
16. Solomon, J C, Selvester, R H and Tolan, G D: An enhanced forward model of the heart. *In* Engineering Foundation Conference. Computerized Interpretation of the Electrocardiogram XI. Bailey, J J, Ed. Engineering Foundation, New York, 1986, p 146
17. Hollenberg, M, Zotlick, J M, Go, M, Yaney, S F, Daniels, W, Davis, R C, Jr and Bedynek, J L: Comparison of a quantitative treadmill exercise score with standard electrocardiagraphic criteria in screening asymptomatic young men for coronary artery disease. N Engl J Med 313(10):600, 1985

J. ELECTROCARDIOLOGY *Supplemental Issue*—OCTOBER, 1987, 8–12

END

FILMED

DATE: 4-92

DTIC